

A multimodal and multimethod assessment of dyadic biobehavioral synchrony in children with autism spectrum disorder

A dissertation proposal submitted to the Personal Health Informatics faculty by

Natasha Yamane
yamane.n@northeastern.edu

October 9, 2024

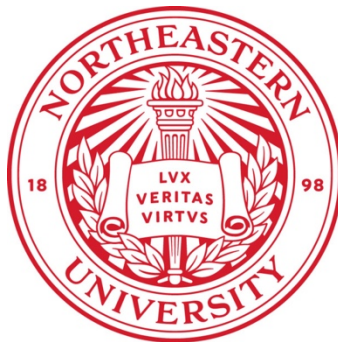


Table of Contents

Abstract	3
1. Introduction	4
2. Related Work	6
2.1. Dyadic Synchrony in Autism Spectrum Disorder	6
2.1.1. Behavioral Synchrony	6
2.1.2. Conversational Synchrony	7
2.1.3. Physiological Synchrony	8
2.2. Approaches to Measuring Parent-Child Synchrony	9
3. Methodology	11
3.1. Participants	11
3.2. Physiological and Behavioral Measures	12
3.2.1. Heart Rate and Heart Rate Variability	12
3.2.2. Physical Proximity	12
3.2.3. Joint Engagement	14
3.2.4. Vocal Turn-Taking	15
3.3. Dyadic Synchrony Measures	16
3.3.1. Linear Techniques	17
3.3.2. Nonlinear Techniques	18
4. Preliminary Work and Feasibility	20
4.1. Physiological Data Quality Assessment and Control	20
4.1.1. Missing Heartbeats	21
4.1.2. Artifactual Heartbeats	21
4.2. Feasibility and Reliability of Data Collection	22
4.2.1. Physical Proximity	23
4.2.2. Joint Engagement	24
4.2.3. Vocal Turn-Taking	25
4.3. Measuring Dyadic Synchrony	26
4.3.1. Descriptive Analyses	27
4.3.2. Dynamic Time Warping	27
4.3.3. Cross-Recurrence Quantification Analysis	30
4.3.4. Cross-Wavelet Analysis	31
4.4. Key Findings and Considerations for Next Steps	35
5. Proposed Timeline	36

Abstract

Dyadic synchrony, the temporal coordination of behavioral and physiological processes in two or more interacting partners, is a phenomenon associated with various relational processes, including social bonding, empathy, prosociality, emotional co-regulation, and teamwork. In autism spectrum disorder (ASD), a neurodevelopmental condition characterized by socio-communicative challenges, there is a nascent, growing body of research that highlights the relevance of dyadic synchrony to uncovering biobehavioral mechanisms associated with social difficulties. Multimodal approaches with different time series techniques to measure dyadic synchrony in individuals with autism, however, remain inadequately explored.

In this dissertation proposal, I present a multimodal and multimethod assessment of physiological and behavioral synchrony in parents and young children with and without ASD. Specifically, I will investigate three types of dyadic synchrony—trend synchrony (TS), concurrent synchrony (CS), and lagged synchrony (LS)—in heart rate and social-communication measures using the following time series techniques: 1) cross-correlation, 2) centered pointwise distance, 3) dynamic time warping, 4) cross-wavelet analysis, and 5) cross-recurrence quantification analysis. I will use standardized parent-report measures of child social responsiveness, moment-to-moment dyadic proximity, joint engagement (JE), and vocal turn-taking, as well as parent and child heart rate (HR) and heart rate variability (HRV), to address the following aims. First, I will perform a validation study by 1) comparing and evaluating the consistency of each TS, CS, and LS measure with other corresponding measures (e.g., TS measure compared to other TS measures), and 2) assessing TS, CS, and LS measures against child social responsiveness and dyadic JE states as ground truth. Following the validation, I will examine within-group associations to explore how dyadic behavioral synchrony (i.e., in vocal turn-taking) relate to those of dyadic physiological synchrony (i.e., in HR and HRV). Next, I will investigate between-group differences in measures of vocal turn-taking synchrony and HR and HRV synchrony between dyads with and without ASD. Finally, I will develop mixed-effects predictive models to assess whether dyadic synchrony of HR, HRV, and vocal turn-taking can reliably predict joint engagement states. Together, findings from my analyses will contribute to greater understanding of the interplay between behavioral and physiological dynamics in autism. With a multimodal and multimethod approach, this dissertation will provide insight into diverse time series techniques to assess dyadic biobehavioral synchrony in autism, informing future work on biomarker identification and intervention development.

1. Introduction

Autism spectrum disorder (ASD) is a lifelong condition now affecting 1 in 36 children (Maenner et al., 2020), characterized by differences in social interaction and communication and by restrictive and repetitive behaviors and interests that manifest in early childhood (American Psychiatric Association, 2013). A growing area of research in autism has emerged over the last decade, focusing on *dyadic biobehavioral synchrony*—the temporal coordination of behavioral and physiological processes in two or more interacting partners (Bernieri & Rosenthal, 1991; Mayo & Gordon, 2020). By studying whether and how physiological and behavioral responses of individuals with ASD are coordinated with those of others during social interaction, researchers can uncover physiological patterns associated with social interactional differences. Importantly, this area of research holds promise for further work on biomarker identification and targeted intervention development.

Dyadic synchrony is ubiquitous across human activities. Pairs of individuals in rocking chairs tend to align their rocks to each other (Richardson et al., 2007), conversation partners match their gestures, language, and facial expressions in time (Louwerse et al., 2012), and mothers and infants synchronize their heart rates during social exchanges (Feldman et al., 2011). Such synchronous behaviors have also been explored with relational outcomes, such as social bonding, empathy, prosociality, and emotional co-regulation (Feldman, 2007; Rennung & Göritz, 2016). At the physiological level, dyadic synchrony is observed in cardiovascular, electrodermal, and neural activities of interaction partners (Palumbo et al., 2017), and is conceptualized to encompass trend, concurrent, and lagged synchrony (Helm et al., 2018). At the behavioral level, dyadic synchrony is observed in verbal (e.g., Duong et al., 2024) and nonverbal behaviors, including gestures, affect, movement, and eye gaze (e.g., Macdonald & Tatler, 2018) with human and non-human (e.g., Griffioen et al., 2020) partners.

Individuals with ASD often exhibit differences in dyadic synchrony processes compared to their typically developing (TD) peers. Research has shown that, compared to TD children, children with ASD show less motor synchronization with partners both spontaneously and as instructed, in activities such as pendulum swinging, chair rocking, clapping, or drumming (Fitzpatrick et al., 2016; Lampi et al., 2020; Marsh et al., 2013; Yoo & Kim, 2018). Other studies have found reduced nonverbal social synchrony in individuals with autism engaged in conversation with other autistic or TD peers (e.g., Georgescu et al., 2020; Glass & Yuill, 2024). When examined with covariates such as ASD severity, dyadic attunement, and partner familiarity, physiological synchrony is also reduced with more child internalizing behavior problems (Wang et al., 2021), greater ASD symptomatology (Baker et al.,

2015), and in interactions with strangers (Saunders Wilder et al., 2018). Such findings point to the idea that differences in dyadic synchrony may underlie social communication and emotional regulation challenges characteristic of ASD. However, research in this area is still nascent.

For dyadic synchrony researchers, choosing the appropriate paradigm and measurement can be a challenge (Levenson, 2024), due to inconsistencies in terminology use and a lack of validated synchrony measures. Existing methods of measuring dyadic physiological and behavioral synchrony involve a range of statistical and time series techniques tailored to capture phenomena also termed “alignment,” “compliance,” “concordance,” “coordination,” “coupling,” “interdependence”, or “linkage” in the literature. These terms are often used interchangeably by researchers, even when referring to different data modalities and employing different analytic approaches. For example, “linkage” is typically used to refer to similarities between physiological signals, while “coordination” is often applied when measuring similarities between behavioral signals.

Commonly used analytic approaches include both linear and nonlinear methods, namely multilevel modeling (e.g., Baker et al., 2015; Wang et al., 2021), cross-correlational analyses (e.g., Capraz et al., 2023; Georgescu et al., 2020), cross-recurrence quantification analysis (e.g., Duong et al., 2024), and wavelet coherence analysis (e.g., Reindl et al., 2022). Such techniques may be used depending on the type of data being considered. Continuous data, such as heart rate, offer a broad range of applicable measurement techniques, some of which are mutually exclusive to continuous data (e.g., wavelet coherence analysis), while others may be amenable to categorical data (e.g., cross-correlations, dynamic time warping).

Building on the approaches and findings of prior work on interpersonal physiological and behavioral synchrony in the typically developing and autistic populations, I will explore the use of both linear and nonlinear time series approaches in measuring trend, concurrent, and lagged biobehavioral synchrony in parent-child dyads with and without ASD. In doing so, I aim to answer the following research questions:

- 1) How consistent are different measures of trend, concurrent, and lagged synchrony when compared to one another?
- 2) Which measures of synchrony can be validated by dyadic joint engagement and child social reciprocity?
- 3) Is physiological synchrony related to behavioral synchrony?
- 4) How do dyadic physiological synchrony and behavioral synchrony differ between dyads with and without ASD?

- 5) Do dyadic physiological synchrony and behavioral synchrony predict joint engagement states in parent-child dyads?

My dissertation is motivated by two key issues. First, there is a diverse range of terminologies and analytic approaches used to refer to and measure interpersonal synchrony in the literature. For the sake of consistency with recent reviews (Carnevali et al., 2024; Glass & Yuill, 2023; McNaughton & Redcay, 2020; Murat Baldwin et al., 2022), I will use “synchrony” to refer to any observed similarities or associations between two partners’ behavioral or physiological signals. Second, research on biobehavioral synchrony in ASD remains limited, with existing studies relying on a narrow range of analytic methods. Overall, these issues leave gaps in our understanding of how different types of synchrony can be measured, manifest, and potentially contribute to social interaction differences in ASD. By employing a multimodal, multimethod approach, my dissertation aims to broaden the range of analytic techniques used to measure dyadic synchrony and provide deeper insights into the physiological and behavioral dynamics that underpin social interaction in both neurotypical children and those with ASD.

2. Related Work

In the following subsections, I review key studies and highlight their synchrony methods and findings that inform the work in my proposal.

2.1. Dyadic Synchrony in Autism Spectrum Disorder

To date, the research corpus on dyadic synchrony in autism spectrum disorder is small, but an increasing number of reviews published in recent years reflects growing interest in the area (Carnevali et al., 2024; Glass & Yuill, 2023; McNaughton & Redcay, 2020; Murat Baldwin et al., 2022). Consensus among reviews reveals three broad areas of synchrony under investigation in the literature: 1) behavioral, 2) conversational, and 3) physiological. Traditionally, measures of dyadic behavioral and conversational synchrony have been obtained manually from video- or audio-recorded interactions by trained and reliable annotators. With advancements in computing power and increased efficiency, researchers now can use validated software to collect the same measures automatically. Below, I summarize the synchrony measures and results of empirical studies investigating dyadic behavioral, conversational, and physiological synchrony in autism.

2.1.1. Behavioral Synchrony

Behavioral synchrony encompasses the coordination of both physical movements and nonverbal behaviors (e.g., gestures, facial expressions, proximity, gaze) during

dyadic social interactions. Four example studies identified in the literature have used manual annotations of social behaviors, as well as motion energy analysis to capture behaviors continuously for synchrony analysis.

Griffioen et al. (2020) used cross-recurrence quantification analysis (CRQA) to measure synchronous movement patterns between children with ASD and Down syndrome and therapy dogs in dog-assisted therapy sessions. CRQA is a nonlinear dynamical analysis technique that quantifies the timing and structure of recurring patterns between two interacting time series using cross-recurrent plots (Zbilut & Webber, 1992; Wallot & Leonardi, 2018; see Section 3.3.2). Child and dog movements (e.g., moving towards the other, stopped moving) were manually annotated by trained and reliable annotators using video recordings of each child-dog dyad. From CRQA, they derived overall proportion of simultaneous movements, as well as recurrence rate, maximum recurrence rate, and recurrence asymmetry within a 30-second window around each recurrence plot's main diagonal. The study found that child-dog synchrony significantly increased from the first to the last therapy session, as reflected in higher overall synchrony, recurrence rates, and maximum recurrence rates. Recurrence asymmetry also showed that children's movements led the dog's movements less in the final session, but this change was not statistically significant.

Three other studies used similar methodological approaches to study the presence and effects of nonverbal behavioral synchrony in child (Glass & Yuill, 2024) and adult (Georgescu et al., 2020; Plank et al., 2023) dyads. In all three studies, the investigators used motion energy as a proxy for dyadic nonverbal communication and windowed (Glass & Yuill, 2024; Georgescu et al., 2020) and non-windowed (Plank et al., 2023) lagged cross-correlations to capture behavioral synchrony. Overall, findings of these studies revealed the following. Among child dyads, dyadic nonverbal behavioral synchrony exists regardless of an ASD diagnostic status, suggesting that children with ASD synchronize to a similar or even greater extent than TD children, depending on the social context and task (Glass & Yuill, 2024). Among adult dyads, synchrony is also present regardless of ASD diagnosis, though it is reduced in dyads with an ASD partner (Georgescu et al., 2020). Moreover, when nonverbal synchrony is led by a TD partner, this leadership creates a positive impression of TD adults, but not of adults with ASD (Plank et al., 2023).

2.1.2. *Conversational Synchrony*

Conversational synchrony focuses on the coordination of verbal and vocal communication, such as turn-taking, speech, and timing during dialogues. This type of synchrony is thought to foster affiliation and facilitate communication, where

more synchrony in verbal behaviors is linked to improved performance on communication tasks (Louwerse et al., 2012; Wadge et al., 2019).

While research on language and conversational patterns in individuals with autism is extensive, studies investigating conversational synchrony in this population are far fewer. Available work in this area has used a combination of manual and automatic methods to annotate linguistic features or synchrony events in transcripts of cross-neurotype (i.e., ASD-TD) dyads. For instance, Hobson et al. (2012) devised a coding scheme to quantify conversational linkage between 12 children with and without ASD and an adult conversational partner. Conversational linkage was manually rated based on the overall back-and-forth exchange of 1) meanings and 2) word utterances in dyads' conversations. Therefore, each dyad was assigned two summary ratings of conversational linkage that did not account for temporal changes in the conversation. The authors found that children in the ASD group demonstrated less conversational linkage with regards to intended meaning in conversation. However, there were no group differences in conversational linkage with regards to word utterances, suggesting that children with and without ASD demonstrate similar patterns in matching word usage with adult partners.

In another study of 82 male adults (65 with ASD), Ochi et al. (2019) used a combination of manual and automatic speech feature extraction methods before quantifying conversational synchrony in their conversations with a study administrator. They manually segmented speech into inter-pausal units and then employed Praat, a popular speech analysis software, to extract prosodic features such as pitch, intensity, and speech rate continuously from conversational transcripts. Synchrony of prosodic features was quantified using windowed cross-correlations of the administrator's and subject's time series. Findings revealed that subjects with ASD exhibited less synchrony in intensity changes, in addition to longer turn-taking gaps and pauses, compared to TD subjects.

2.1.3. *Physiological Synchrony*

Physiological synchrony refers to the synchronization of neural and autonomic processes, including cardiac and electrodermal activity (EDA), between individuals engaged in social interaction. Research on dyadic physiological synchrony in ASD is still nascent. To the best of my knowledge, Baker et al. (2015) were the first to investigate physiological synchrony in dyadic interactions involving individuals, particularly parents and children, with ASD. Since then, only two other studies on parents and children with ASD have been reported (Saunders Wilder et al., 2018; Wang et al., 2021). Around the same time, Dunsmore et al. (2019) also examined physiological synchrony in a proof-of-concept study with adult dyads with ASD.

Across these studies, two focused on electrodermal activity (Baker et al., 2015; Saunders Wilder et al., 2018) and two focused on cardiac activity (Dunsmore et al., 2019; Wang et al., 2021). To measure synchrony, all studies used either hierarchical linear or dynamic systems modeling.

Baker et al. (2015) investigated wrist-recorded EDA synchrony in 28 parent-child dyads with ASD (mean child age: 6.7 years). Each parent and child wore an Affectiva Q sensor (Poh et al., 2010) that recorded EDA and acceleration continuously while they engaged in naturalistic free play with toys. The authors used a hierarchical linear model (HLM) to capture the effects of both time-varying (i.e., EDA, acceleration) and non-time-varying factors (e.g., ASD symptomatology). Results of the study showed that parent-child EDA synchrony was positively correlated with observed parent-child attunement and lower ASD severity in the child.

Following the same HLM approach above, Saunders Wilder et al. (2018) explored EDA synchrony in 30 children with and without ASD (8 with ASD) engaged in semi-structured free play with their parent and ADOS tasks with an examiner. Parent-child EDA synchrony was found to be partially moderated by children's social reciprocity as measured by the second edition of the Social Responsiveness Scale (SRS-2; Constantino & Gruber, 2012). Additionally, EDA synchrony varied depending on whether the child was interacting with their parent or examiner.

Most recently, Wang et al. (2021) used HLMs to explore associations between dyadic interaction quality and child behavioral problems with cardiac—specifically respiratory sinus arrhythmia (RSA)—synchrony in 74 parent-child dyads with and without ASD (31 with ASD). Dyads were tasked to engage in a joint drawing task together, while their ECGs were recorded with the Biopac MP150 system. Their results showed that TD children showed stronger positive RSA synchrony with their parents than children with ASD. RSA synchrony magnitude was also greater in dyads with higher ratings of interaction quality and when children with ASD had lower internalizing problems.

2.2. Approaches to Measuring Parent-Child Dyadic Synchrony

Research on parent-child dyadic synchrony is expanding and builds on foundations laid by pioneers in dyadic developmental psychology, who have explored dynamic, moment-to-moment coordination between mothers and infants (Cohn & Tronick, 1987; Jaffe et al., 2001; Stern et al., 1975; Tronick & Cohn, 1989). With the growing commercial availability of biosensor systems, there is also increased interest in integrating physiological and behavioral data to provide a more comprehensive understanding of how synchrony in both domains contributes to social developmental and affective outcomes (Feldman, 2007). Further, advancements in

computing power have enabled researchers to employ more sophisticated analytic techniques that achieve more nuanced quantifications of dyadic synchrony.

Building on the foundational work above, Feldman and her colleagues were among the first to rigorously examine biobehavioral mechanisms underlying emotional bonding, social development, and autonomic regulation in the parent-child dyad. By integrating both behavioral and physiological data, Feldman et al. (2011) revealed how early parent-infant interactions—characterized by mutual gaze, vocalization synchrony, and affect synchrony—are closely linked to cardiac synchrony. In their study, events of interactional synchrony were annotated via microanalysis of face-to-face interactions between 40 mothers and their healthy infants. Cardiac synchrony was quantified using lagged cross-correlation analyses of mother and infant interbeat intervals (IBIs). Their analyses revealed the presence of leader-follower dynamics in mother-infant IBI synchrony, where mothers and infants adapt their heart rhythms to those of each other's within lags of less than 1 second. Further, interactional synchrony measures that were most effective at increasing IBI synchrony were vocalization synchrony ($R = .096$, $p < .001$) and affect synchrony ($R = .090$, $p = .004$).

Cross-correlations, among other methods such as multilevel modeling, are commonly employed to investigate parent-child synchrony in cardiac and electrodermal activity (DePasquale, 2021). For instance, in a recent study by Capraz et al. (2023), cross-correlation analyses with time lags of -3 to +3 seconds were used to examine the relationship between mother-child IBI and respiratory sinus arrhythmia synchrony and their associations with positive facial affect. Their findings revealed that both IBI and RSA synchrony were higher during interactive tasks compared to control conditions, and individual and shared positive affect were associated with higher IBI and RSA synchrony during the interactive tasks. Notably, effects of positive facial affect on cardiac synchrony were only observed within and not across dyads, and specifically when examining individual mother and child positive affect, rather than shared affect.

Simultaneously, additional studies of parent-child RSA synchrony using multilevel modeling and coupled autoregressive analyses exist. While these models have revealed insights into parent-child RSA synchrony, they differ from the time series methods used in this proposal and thus will not be reviewed here. For a meta-analysis of these studies and their methods, refer to Miller et al. (2022).

A less common approach gaining greater use with parent-child cardiac data is cross-wavelet analysis, adapted from neural synchrony studies to capture time-frequency relationships in dynamic signals. Reindl et al. (2022) used wavelet coherence

analyses to capture mother-child and stranger-child synchrony in functional near-infrared spectroscopy and IBI data collected during cooperative and competitive tasks. They found that while neural synchrony was higher in mother-child pairs compared to stranger-child dyads, IBI synchrony did not show this distinction. Neural and cardiac synchrony were also positively related during competitive but not cooperative tasks, suggesting that different systems may reflect distinct, context-dependent synchrony processes.

Meanwhile, researchers investigating areas beyond psychophysiology, such as movement (e.g., López Pérez et al., 2017) and conversation (e.g., Duong et al., 2024), in the parent-child dyad, have applied cross-recurrence quantification analysis. Using motion energy analysis to capture continuous movement patterns in 21 parent-infant dyads, López Pérez et al. (2017) applied CRQA to assess the coordination of infants' head movements and parents' hand movements while holding a toy during face-to-face play. Main findings showed that higher levels of parent-infant movement synchrony were associated with more coordinated and engaging interactions.

Duong et al. (2024) also used CRQA on categorical conversational data in 124 parent-child dyads to study links between parent-child alignment in number talk utterances and children's math skills. Transcripts of conversational data were automatically annotated and then manually reviewed with binary occurrences of number talk based on a prior coding scheme. Their CRQA revealed several metrics that were positively linked with parent-child number talk frequency, but only recurrence rate was significantly related to children's math skills. Overall, this suggests that reciprocity in parent and child number talk may influence or reflect early math abilities more than simple exposure to number talk in children.

3. Methodology

In the following subsections, I describe the subset of physiological, video, and audio data from the enTRAIN study that I will use for my dissertation. The enTRAIN study, conducted by the Computational Behavioral Science Lab at Northeastern University in collaboration with colleagues at the MIT Media Lab, investigates links between socio-affective behavior and dyadic autonomic physiology in children with and without ASD and their parents. I also discuss the analytic approaches I will use to measure dyadic synchrony.

3.1 Participants

A total of 35 parent-child dyads (24 TD and 11 with ASD) participated in the original enTRAIN study. Parents and children were asked to engage in a series of

standardized social-emotional regulation tasks while wearing two wireless physiological devices: the Affectiva Q Sensor and Actiwave Cardio. The Q Sensor is a wrist-worn device that captures skin conductance, skin surface temperature, and 3D motion, and has been validated against commercial laboratory sensors (Poh et al., 2010). The Actiwave Cardio, from CamNtech, is a chest-worn electrocardiography (ECG) and accelerometry device that has shown good reliability and validity when compared to gold-standard cardiovascular measures (Kristiansen et al., 2011). Due to the unavailability of complete ECG data for one TD dyad and video data for three TD dyads, the final sample includes data from 20 TD dyads, with a mean child age of 3.7 years ($SD = 1.1$), and 11 dyads with ASD, with a mean child age of 4.3 years ($SD = 1.1$). For my dissertation, I will use ECG, video, and audio data recorded during the 15-minute ‘Dyadic Play’ task. In this task, parent-child dyads were provided with the same set of toys and instructed to play together as they would at home. This task was selected for its relatively longer duration and more naturalistic context compared to the other tasks. Each dyad was video-recorded with five different wide-angle lens cameras in the study room.

3.2 Measures

I will use a combination of automatic and manual methods to extract cardiac (i.e., heart rate, heart rate variability) and nonverbal social behavioral data (i.e., physical proximity, joint engagement, vocal turn-taking) from each parent-child dyad in the enTRAIN study.

3.2.1 Heart Rate and Heart Rate Variability

Parent and child ECG data were collected at a sampling rate of 1024 Hz with the Actiwave Cardio. Raw ECG data is pre-processed in Python with the PhysioView pipeline (formerly called HeartView; Yamane et al., 2024) for heart rate (HR) and heart rate variability (HRV) feature extraction with the FLIRT package (Föll et al., 2021). PhysioView provides functions to perform all necessary ECG pre-processing procedures (see Section 4.1), namely signal filtering, heartbeat detection, data quality assessment, and artifactual beat correction. Interbeat intervals, derived from detected heartbeats, are then resampled using cubic spline interpolation every 250 ms and converted into HR values by dividing the IBI values from 60,000. Raw IBI values are used as input for FLIRT’s HRV feature extraction methods to calculate time-domain HRV features such as the root mean square of successive differences (RMSSD) across 60-second windows with a 59-second overlap. The RMSSD is the primary time-domain measure used to estimate beat-to-beat variance in HR as a function of the parasympathetic nervous system. Higher RMSSD values typically

correspond to greater autonomic adaptability compared lower values (Shaffer & Ginsberg, 2017).

3.2.2 Physical Proximity

Physical proximity is derived with pose and depth estimation, both of which are computer vision techniques that enable 3D spatial information to be extracted from anatomical key points detected from people in images or videos. Pose estimation algorithms identify the locations of specific body landmarks, such as joints and extremities, to infer the spatial arrangement and movement of individuals. To this end, I will use Google's TensorFlow library with the multi-pose MoveNet model (Bajpai & Joshi, 2021) for two-dimensional (2D) pose estimation and Intel's MiDaS model (Ranftl et al., 2020) for depth estimation. The MoveNet model is designed to detect and track the positions of multiple people within a single image or video frame using high-precision estimates of 17 anatomical key points (Figure 1) based on Microsoft's Common Objects in Context (COCO) dataset (Lin et al., 2014). The MiDaS model is a depth estimation model that predicts the relative distance of each pixel in an image from the camera, providing depth maps that represent the three-dimensional (3D) structure of the scene.

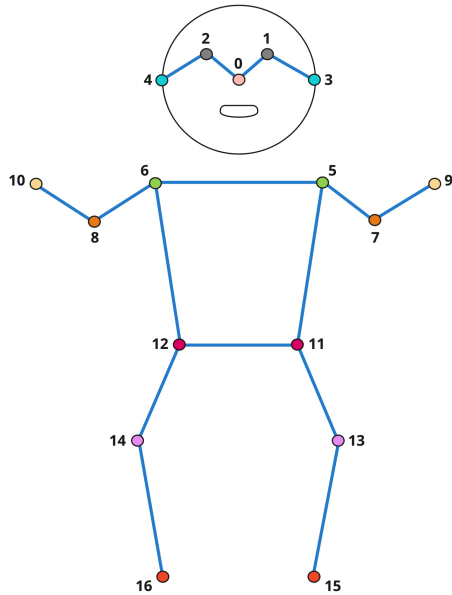


Figure 1. Anatomical key points for pose estimation. Numbers above correspond to the following unique anatomical landmarks used for pose estimation: 0 = Nose; 1 = Left eye; 2 = Right eye; 3 = Left ear; 4 = Right ear; 5 = Left shoulder; 6 = Right shoulder; 7 = Left elbow; 8 = Right elbow; 9 = Left wrist; 10 = Right wrist; 11 = Left hip; 12 = Right hip; 13 = Left knee; 14 = Right knee; 15 = Left ankle; 16 = Right ankle.

Proximity is calculated as the Euclidean distance between the centroids of parent and child, where each person's centroid is represented by x , y , and z coordinates calculated as the averages of the 3D coordinates of detected key points in their respective planes. To ensure consistency across all parent-child dyads, I will use video data recorded from the same perspective with the same wide-angle GoPro HERO5 Black camera used in the original study. For each frame, each person's 3D coordinates are derived from their 2D key points using their corresponding depth values generated by a MiDaS depth map, along with focal length and optical center values (Hartley & Zisserman, 2004) intrinsic to the GoPro HERO5 Black. The relative distance between the 3D coordinates of the parent's and child's centroids is calculated according to Equation 1 and then normalized with min-max normalization.

$$\text{Proximity} = \sqrt{(x_{\text{parent}} - x_{\text{child}})^2 + (y_{\text{parent}} - y_{\text{child}})^2 + (z_{\text{parent}} - z_{\text{child}})^2} \quad (1)$$

3.2.3 Joint Engagement

Joint engagement emerges when a child begins to include a caregiver in their interaction with an object. Joint engagement (JE) is a critical developmental process because it allows children to learn through shared experiences and interactions with others, facilitating their understanding of the social world. Based on the State-Based Joint Engagement coding scheme (Adamson et al., 2004; Bakeman & Adamson, 1984), two distinct joint engagement states—*Supported* and *Coordinated* joint engagement—are identified and annotated from each video-recorded ‘Dyadic Play’ task. Operational definitions and examples of Supported and Coordinated JE are given in Table 1.

Table 1. Operational Definitions of Joint Engagement States

Type	Operational Definition	Example
Supported	Occurs when the child and caregiver are engaged with the same object/activity, but the child does not coordinate their attention between the object and the caregiver. The caregiver structures the interaction by providing scaffolding (e.g., verbal prompts, physical guidance, gestures) to maintain the child's attention on the shared activity.	While reading together, the caregiver talks about the pictures in a book and points things out, maintaining the child's interest, but the child remains focused on the book rather than the caregiver.

Coordinated	The child attends to the shared object/activity and also coordinates their attention between the object and their caregiver. There is explicit evidence that the child demonstrates responsiveness to the caregiver (e.g., eye contact, gestures).	While playing with a toy car, the child looks at the car and then the caregiver to see their reaction. The caregiver smiles and gives verbal encouragement. The toddler smile, and pushes the car again, while looking up at the caregiver.
-------------	--	---

3.2.4 Vocal Turn-Taking

Patterns of vocal turn-taking are inferred from vocal states annotated with the Jaffe-Feldstein Model of Dyadic Vocal Rhythm ([Jaffe & Feldstein, 1970](#)). This model has been adapted for use with parent-child data ([Jaffe et al., 2001](#)) and focuses on the timing and coordination of vocalizations by social partners in conversation. Thus, five vocal states can emerge from different sequences of vocalizations and silences observed between two social partners (see Figure 2):

1. *Vocalization (V)*, defined as a continuous utterance of a speaker containing no silence greater than 250 ms in duration.
2. *Pause (P)*, defined as a joint silence greater than or equal to 250 ms in duration and bounded by the vocalizations of the speaker.
3. *Switching pause (SP)*, defined as a joint silence greater than or equal to 250 ms in duration and initiated by a speaker, but terminated by a vocalization of their social partner. Switching pauses are assigned to the speaker whose turn it terminates.
4. *Non-interruptive simultaneous speech (NSS)*, defined as a simultaneous occurrence of vocalizations by both social partners that begins and ends while the turn-holding partner vocalizes continuously.
5. *Interruptive simultaneous speech (ISS)*, defined as a simultaneous occurrence of vocalizations by both social partners that is initiated while the turn-holding partner is vocalizing, but continues after they stop.

Using Audacity, a free and open-source multi-track audio editor and recorder, each dyad's audio data is first pre-processed with noise reduction and split into one audio track each for the parent and child. Segments of non-vocalizations in each track are converted into silences, leaving only segments considered to be communicative vocalizations (i.e., speech, laughter, sighs, exclamations, and hums). Each edited parent and child track is then exported in MP3 format with an 8000-Hz sampling rate and processed in Python for vocal state extraction.

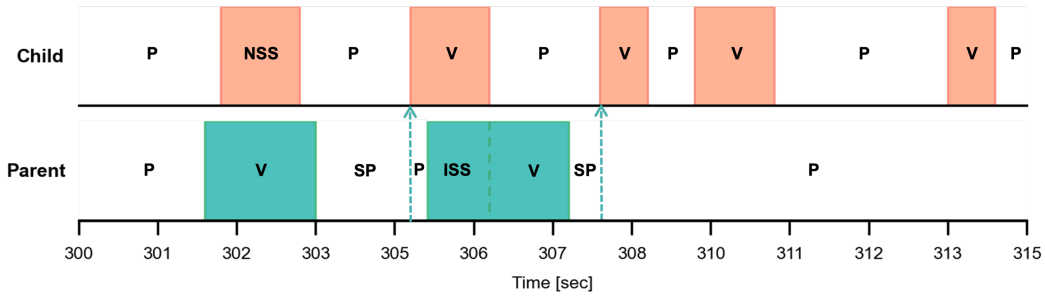


Figure 2. Example interactional sequence of vocal states between a parent and child. V = vocalization; P = pause; SP = switching pause; NSS = non-interruptive simultaneous speech; ISS = interruptive simultaneous speech. Arrows pointing up denote the end of the parent’s turn.

Two higher-level features of vocal turn-taking are then extracted from specific sequences of vocal states for each partner: a *switching turn*—the beginning of a partner’s vocalization until the end of their switching pause—and an *interruptive turn*—the beginning of a partner’s interruptive simultaneous speech occurrence until the beginning of theirs or the other partner’s next vocalization. Labeling of each type of vocal turn precludes any overlap between switching turns and interruptive turns in each partner’s time series.

3.3 Dyadic Synchrony Measures

I will measure three types of dyadic synchrony, as defined in work by Helm et al. (2018) and Denk et al. (2024)—trend, concurrent, and lagged synchrony. **Trend synchrony** refers to the alignment of overall patterns or long-term changes in two signals, focusing on whether they follow similar trajectories over time. **Concurrent synchrony** refers to the simultaneous, moment-to-moment fluctuations around a trend between two signals, measuring how closely they vary in tandem at each time point. **Lagged synchrony** refers to the temporal relationship between signals, assessing how much one signal leads or follows the other over a given time lag. I aim to capture each type of synchrony between parent and child physiological and behavioral signals using linear and nonlinear time series approaches (Table 2). These approaches offer varying capacities to measure one, two, or all three synchrony types. Unified approaches capturing all three synchrony types are cross-wavelet analysis and cross-recurrence quantification analysis.

Table 2. Time Series Approaches to Measuring Dyadic Synchrony

Approach	Synchrony Type(s)	Data Type(s)	Has Temporal Resolution
<i>Linear Approaches</i>			
Cross-correlation	Concurrent; Lagged	Continuous; Categorical	Yes*
Centered pointwise distance	Concurrent; Lagged	Continuous	Yes
<i>Nonlinear Approaches</i>			
Cross-wavelet analysis	Trend; Concurrent; Lagged	Continuous	Yes
Cross-recurrence quantification analysis	Trend; Concurrent; Lagged	Continuous; Categorical [†]	No
Dynamic time warping	Trend	Continuous; Categorical [†]	No

* Temporal resolution can be created via windowing.

[†] A custom distance function must be used.

3.3.1 Linear Techniques

Linear techniques are commonly employed to assess concurrent and lagged synchrony between two time series. These techniques are grounded in the assumption that changes in one signal can be linearly related to changes in another signal, allowing for straightforward interpretations of their interactions. I will use two linear techniques—**cross-correlation** and a time series distance measure from Denk et al. (2024) that I have termed **centered pointwise distance (CPD)**—to capture concurrent and lagged synchrony between parent and child HR, HRV RMSSD, and vocal turn-taking.

Cross-correlation. Cross-correlation is a commonly used method to assess synchrony between and within individuals (e.g., Chatel-Goldman et al., 2014; Chen et al., 2023; Feldman et al., 2011). It measures the degree to which two signals are correlated at different time lags, indicating how much one signal may lead or lag behind the other. Peaks in the cross-correlation function represent time lags where the signals are most synchronized, providing insight into whether their interactions occur

simultaneously or are offset by some lag. Negative lags indicate that the second partner, whose signal is represented as $Y(t)$, leads the interaction, while positive lags suggest that the first, represented as $X(t)$, is leading.

Centered pointwise distance. Centered pointwise distance (CPD) is a time series distance measure presented in work by Denk et al. (2024) to measure dyadic cardiac synchrony. This approach quantifies the distance between two continuous time series at corresponding time points with or without lags, providing a measure of concurrent or lagged synchrony. In CPD, both time series are first centered by subtracting their respective mean value, resulting in only deviations from their averages. The absolute difference (i.e., distance) between the two time series is then calculated at each time point. Lower distance values indicate closer alignment or greater synchrony between the two centered signals.

3.3.2 Nonlinear Techniques

Nonlinear techniques can capture state-dependent dynamics and more complex temporal patterns of dyadic synchrony that may be missed by linear approaches. For example, nonlinear techniques can identify periodic oscillations or chaotic behavior that reflect how the interaction between two time series evolves over time. Thus, nonlinear techniques are robust in the presence of non-stationary processes whose relationship may change over time. I will use three nonlinear approaches—**dynamic time warping**, **cross-recurrence quantification analysis**, and **cross-wavelet analysis**—to measure trend, concurrent, and lagged synchrony.

Dynamic time warping. Dynamic time warping (DTW) is a time series distance technique used to measure the similarity between two time series by aligning them in a way that minimizes the overall alignment cost (Vintsyuk, 1968). This cost represents the cumulative difference between the aligned points of the time series, allowing for nonlinear stretching or compression along the time axis to account for differences in timing or pacing. Thus, DTW can be useful when comparing sequences that may vary in length or speed. The primary outcome measure relevant to trend synchrony is the *alignment cost* between two partners' time series, with a lower alignment cost indicating greater synchrony between the two partners.

Cross-recurrence quantification analysis. Cross-recurrence quantification analysis (CRQA) is a nonlinear method for determining synchrony between two time series. In CRQA, cross-recurrence plots are used to visualize dyadic synchrony by depicting where trajectories in the phase space of one time series recur in the phase space of another (Zbilut & Webber, 1992; Marwan et al., 2002; Wallot & Leonardi, 2018). Key parameters in CRQA include the embedding dimension (M), time delay (D), and the fixed radius (r) that are critical for reconstructing each time series' phase space and

determining similarity between two time series. Commonly used outcome measures derived from CRQA include the recurrence rate, determinism, entropy, average diagonal line length, and maximum diagonal line length. *Recurrence rate* measures overall synchrony, expressed as the proportion of points where trajectories of partners' time series recur. *Determinism* reflects the regularity or extent of predictability in recurrent patterns. *Average and maximum diagonal line lengths* assess the persistence and duration of synchrony, showing how long the time series maintain consistent patterns of interaction. Lastly, *entropy* indicates the degree of irregularity in recurrent patterns, where higher entropy values suggest less predictable interactions between two partners, and lower entropy values suggest more regular synchrony.

Cross-wavelet analysis. Cross-wavelet analysis is a method for examining the relationships between two continuous time series in both time and frequency domains, revealing both their *wavelet coherence* and the *phase angle differences*. In this approach, a continuous wavelet transform is first applied to each signal. This process involves the convolution of each signal with daughter wavelets—scaled and shifted versions of a mother wavelet (commonly the Morlet wavelet)—to capture how much of a daughter wavelet's shape is present in the signal across time (Torrence & Compo, 1998). This is represented as one wavelet coefficient per time point and frequency band for each signal. Next, the wavelet coefficients of one signal are multiplied by the complex conjugate of the other, producing the cross-wavelet transform and its magnitude, known as cross-wavelet power. *Wavelet coherence* is then calculated by normalizing the cross-wavelet power according to Equation 2, where S denotes a smoothing operator applied to reduce noise and W represents the wavelet coefficients of the two signals X and Y at scale a and time point b (Grinsted et al., 2004). Resulting coherence values range from 0 to 1, with higher values indicating a stronger correlation between the two signals at specific frequencies and times.

$$R^2(a, b) = \frac{|S(W_{XY}(a, b))|^2}{S(|W_X(a, b)^2|) \cdot S(|W_Y(a, b)^2|)} \quad (2)$$

Important to measuring trend and concurrent synchrony are coherence values at specific frequencies. Notably, coherence at *low* frequencies (typically 0.04 to 0.15 Hz) measure trend synchrony, and coherence at *high* frequencies (0.15 to 0.4 Hz) measure concurrent synchrony. Lastly, *phase angle differences*, which can be calculated after obtaining the cross-wavelet transform, measure lagged synchrony, where positive phase differences indicate that one signal leads the other, and negative phase differences suggest that it lags behind the other.

4. Preliminary Work and Feasibility

In preparation for my dissertation, preliminary work has focused on establishing the reliability of physiological and behavioral data collected in the enTRAIN study, as well as the feasibility of applying the abovementioned time series techniques to measuring parent-child synchrony. In the following subsections, I present preliminary findings on several key areas. First, I describe and present results of my quality assessment of cardiac data collected from the enTRAIN study. Next, I discuss the reliability and feasibility of collecting behavioral measures from video and audio data of two pilot dyads that I selected based on results of my ECG quality assessment. Finally, I provide three examples of measuring dyadic biobehavioral synchrony on the same pilot data.

4.1 Physiological Data Quality Assessment and Control

Physiological data quality assessment and control is integral to the validity and reliability of physiological measures used in this dissertation. Because modern wearable systems are portable and smaller than their traditional, larger stationary counterparts, their signals are more susceptible to corruption by artifacts. As a result, signal quality assessment procedures that involve detecting and evaluating artifacts and missingness based on expected signal characteristics have become an increasingly important step during and after data collection.

Motivated by the need for a well-documented, freely accessible tool to assess the suitability of wearable biosensor data for further pre-processing and analyses in research, I have developed and continually refined a software package initially known as HeartView—now called PhysioView. PhysioView is an open-source Python package that leverages state-of-the-art algorithms to quantify artifactual, missing, and invalid data from electrocardiograph, photoplethysmograph, and electrodermal activity recording devices. In addition to these capabilities, PhysioView includes specialized modules and a web interface for pre-processing, visualization, and correction of cardiac and EDA data. In prior work ([Yamane et al., 2024](#)), PhysioView’s cardiac data quality metrics have been validated and evaluated on the enTRAIN dataset and the publicly available WESAD dataset ([Schmidt et al., 2018](#)). These metrics include numbers of missing and artifactual beats per segment and segments with an invalid number of beats. Across 60-second segments, I have computed proportions of missing and artifactual beats in each cardiac recording collected in the enTRAIN study.

4.1.1 Missing Heartbeats

PhysioView determines the number of missing beats against an expected number of beats in a given segment. The pipeline calculates the expected number of peaks by computing the median of second-by-second HR values, which are derived using the harmonic mean of HR values over a 2-second window (Graham, 1978). The number of missing beats is then calculated as the difference between the expected number and number of detected beats.

Descriptive statistics of the proportions of missing beats per segment were calculated separately for ECG recordings of dyads with ASD and TD dyads. On average, ECG data of children with ASD contained 20.6% missing beats per segment, and ECG data of TD children contained 4.7% missing beats per segment. ECG data of parents in the ASD group contained 8.5% missing beats per segment, and ECG data of parents in the TD group contained 6.3% missing beats per segment. Figure 3 displays the distributions of mean proportions of missing beats across all segments per parent and child by group.

4.1.2 Artifactual Heartbeats

PhysioView provides two time domain-based artifact identification methods for cardiac data (Berntson et al., 1990; Hegarty-Craver et al., 2018). To conservatively evaluate and avoid false negatives in detecting the number of artifactual beats per 60-second segment in the enTRAIN data, I used both artifact identification methods.

Berntson et al.'s (1990) criterion beat difference test marks beats as artifacts if their respective IBIs exceed a criterion beat difference score multiplied by a tolerance value that adjusts the sensitivity of artifact identification. For each IBI, a criterion

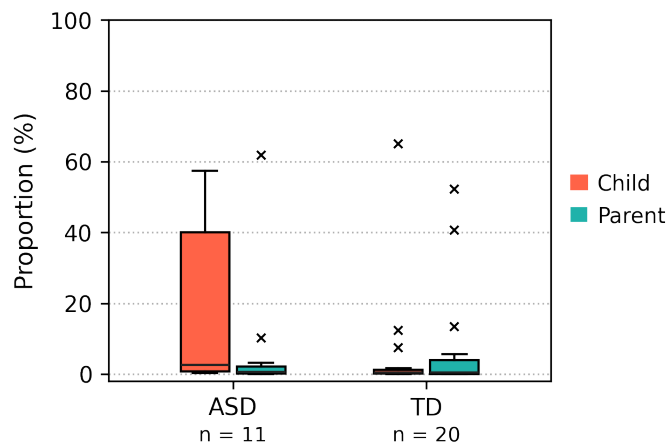


Figure 3. Mean proportions of missing beats per 60-second segment by group.

beat difference score is calculated using the maximum expected difference and median of its six neighboring IBIs, where the maximum expected difference is determined using the quartile deviation of the IBI and its neighbors. This approach has been used to pre-process ambulatory cardiac data in multiple studies (e.g., Hilty et al., 2022; Hoemann et al., 2020; Menghini et al., 2019). Similarly, Hegarty-Craver et al.'s (2018) artifact identification method flags IBIs as artifactual if they fall outside of the acceptable range of approximately 80% to 140% of a dynamically estimated IBI. For each IBI, the dynamically estimated IBI is calculated as the rolling median of the preceding six IBIs.

On average, ECG data of children with ASD contained 54.7% artifactual beats per segment, and ECG data of TD children contained 32.7% artifactual beats per segment. ECG data of parents in the ASD group contained 33.3% artifactual beats per segment, and ECG data of parents in the TD group contained 49.0% artifactual beats per segment. Figure 4 displays the distributions of mean proportions of artifactual beats across all segments per parent and child by group.

4.2 Feasibility and Reliability of Behavioral Data Collection

Feasibility and reliability of collecting behavioral measures were assessed on pilot dyads selected based on ECG quality assessment results with PhysioView. One dyad with ASD ('A02'; child age: 3.6 years) and one TD dyad ('T21'; child age: 3.9 years) were selected based on criteria that required less than 50% artifactual beats and less than 20% missing beats per 1-minute segment in their ECG data. Artifactual and missing beats were initially corrected using PhysioView's automated beat correction algorithm, with any remaining uncorrected beats manually corrected with visual inspection in Python. Corrected beats were used to compute HR resampled at 4 Hz

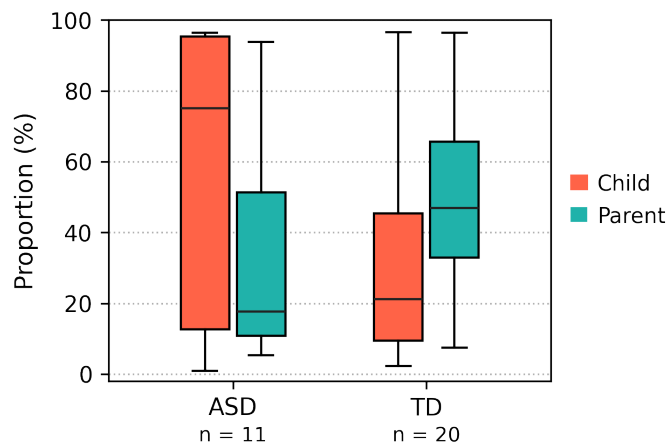


Figure 4. Mean proportions of artifactual beats per 60-second segment by group.

with cubic interpolation and to extract HRV RMSSD values across 60-second sliding windows with 59-second overlaps (i.e., at a sampling rate of 1 Hz).

4.2.1 Physical Proximity

Three-dimensional pose estimation and dyadic proximity calculation for each dyad during ‘Dyadic Play’ was performed in Python. The program uses OpenCV, TensorFlow, the multi-pose MoveNet model ([Bajpai & Joshi, 2021](#)), and the MiDaS model ([Ranftl et al., 2020](#)) to extract x -, y -, and z -coordinates of each person’s anatomical key points every quarter second. First, the program leverages the MoveNet model to detect up to 17 two-dimensional key points on each of the parent and child while assigning confidence scores ranging from 0 to 1. To maximize key point detection, I selected a confidence score threshold of 0.3, thus keeping only detected key points with confidence scores of at least 0.3. For each key point that met the threshold criterion, the program uses the MiDaS model to estimate its depth from the camera’s viewpoint and convert its 2D coordinates into 3D coordinates for proximity calculation (see Section 3.2.2).

While automated, this task is time-intensive, given 1) the amount of video data recorded for each dyad’s ‘Dyadic Play’, and 2) the use of two deep-learning models that require substantial computational resources to process high-dimensional data and perform feature extraction. In pilot data using a sampling interval of 0.25 second, 3,672 video frames were extracted and processed for dyad ‘A02’ and 3,897 frames for dyad ‘T21’. On average, 3D pose estimation took 36.6 minutes to complete on each dyad’s respective frames when performed on a MacBook Pro with a 1.4 GHz Intel Core i5 processor and 8 GB of RAM. Multiprocessing, a technique that leverages multiple CPU cores to perform tasks simultaneously, could significantly reduce the total time required to perform this task on the remaining enTRAIN dyads’ video files. Descriptive analysis of dyads’ normalized proximity values over time revealed that dyad ‘A02’ displayed greater variability in proximity behaviors compared to dyad ‘T21’ (Figure 5). This observation is consistent with previous work showing greater interpersonal distancing behaviors in children with ASD ([Gessaroli et al., 2013](#)), particularly in relation to autism severity ([Budman et al., 2019](#)).

Despite the robustness of the deep-learning models employed, certain limitations in data capture are inevitable. Approximately 25.5% of the video frames processed for each dyad was missing proximity data due to undetected points on either the parent or child, who was out of frame or obscured by objects or each other. This data loss underscores challenges posed by contexts in which participants’ natural movements can prevent critical visual information from being captured. Addressing this issue

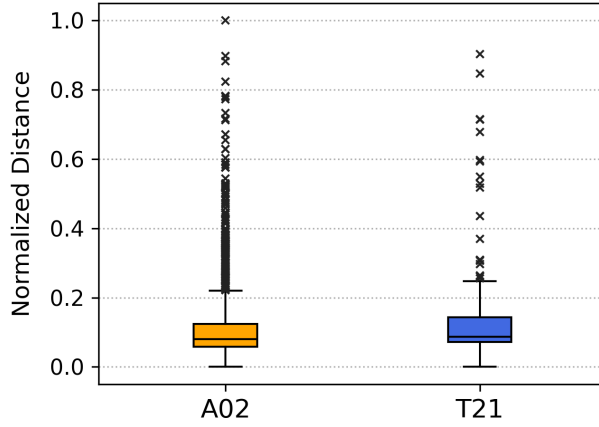


Figure 5. Distributions of dyadic proximity in pilot data.

may require more sophisticated models capable of handling occlusions. As my project progresses, I will explore strategies to handle these missing data points to ensure the reliability of dyads' proximity data.

4.2.2 *Joint Engagement*

Annotating Supported and Coordinated JE states in video data of parent-child dyads is feasible, yet time-intensive. All video annotations are done without audio in the open-source video annotation software Datavyu ([Datavyu Team, 2014](#)). Training for reliability took approximately six weeks, during which another research assistant and I independently annotated video data of nine randomly selected parent-child dyads from the enTRAIN study, while being blinded to each dyad's diagnostic status. Each dyad's video-recorded interaction lasts approximately 15 minutes and takes anywhere between 45 minutes and 1 hour and 15 minutes to annotate. After each video was annotated, reliability statistics were calculated, discrepant codes were reviewed with corresponding video footage, and operational definitions and behavioral examples were discussed and refined (see Section 3.2.3 for details). Reliability was evaluated using percentage of agreement and Gwet's agreement coefficient (AC_1 ; [Gwet, 2008](#)) on annotations of JE states in 1-second intervals. The AC_1 statistic was selected over Cohen's kappa due to its robustness against skewed label distributions that can lead to small kappa values despite large percentages of interrater agreement ([Dettori & Norvell, 2020](#); [McHugh, 2012](#)). We were required to achieve at least 80% average agreement on both Supported and Coordinated JE states and an agreement interpretation of at least 'Moderate,' based on the coefficient's cumulative probability of falling within that benchmark range with a cutoff of 95% ([Gwet, 2008](#)). This process was repeated until adequate reliability was achieved on

$n = 7$ dyads, approximately 20% of the study sample. Reliability statistics of the seven dyads whose JE data achieved adequate reliability are shown in Table 3.

Table 3. Inter-Annotator Reliability of Joint Engagement States

Blinded ID	$AC_1 \pm SE$	Agreement	Cumulative Probability	Interpretation
2294	.82 ± .06	92.38	.99	Good
2292	.57 ± .38	86.40	.99	Moderate
2318	1.00 ± .06	90.57	.99	Good
1663	1.00 ± .08	88.21	.99	Moderate
2355	.92 ± .06	90.39	.99	Good
2589	.99 ± .08	90.59	.99	Moderate
2623	.85 ± .05	89.20	.99	Good

Descriptive analysis of the frequencies and durations of JE states observed in the pilot dyads (Table 4) revealed a few key findings that are congruent with the literature on parent-child dynamics in ASD (e.g., Freeman & Kasari, 2013; Patterson et al., 2014). On average, dyad ‘A02’ spent less time in both Supported ($M = 45.8$ sec, $SD = 36.5$) and Coordinated ($M = 3.0$ sec, $SD = 1.0$) JE than dyad ‘T21’ (Supported: $M = 88.4$ sec, $SD = 85.1$; Coordinated: $M = 29.7$ sec, $SD = 27.9$). Additionally, although dyad ‘A02’ spent less time in both types of JE, they entered Supported JE more often than dyad ‘T21’. Together, these results suggest more frequent and shorter moments of parent-initiated or sustained engagement by dyad ‘A02’ than by dyad ‘T21’.

Table 4. Descriptive Statistics of Joint Engagement Frequency and Duration

Dyad	Supported			Coordinated		
	Frequency	Duration (sec)		Frequency	Duration (sec)	
		$M \pm SD$	Mdn, IQR		$M \pm SD$	Mdn, IQR
‘A02’	12	45.8 ± 36.5	39.0, 29.3	2	3.0 ± 1.0	3.0, 1.0
‘T21’	8	88.4 ± 85.1	39.5, 120.0	3	29.7 ± 27.9	13.0, 31.0

4.2.3 Vocal Turn-Taking

While not yet reliable between annotators, the process of annotating vocal states is also feasible with Audacity. Because the process is done through a “reverse-annotation” approach, whereby annotators are required to generate silences during non-vocalization segments, rather than explicitly labeling vocalization occurrences in audio files (see Section 3.2.4), I expect the annotator training period to take no

more than a few weeks. I have already prepared Audacity project files, each 10 minutes in length, of $n = 7$ randomly selected dyads for inter-annotator reliability.

With regards to the pilot data (Table 5), both the parent and child in dyad ‘A02’ exhibited lower ratios of switching-to-interruptive turn frequency compared to the parent and child in dyad ‘T21’. Further, a ratio of 61:25 for parent switching-to-interruptive turn frequency in dyad ‘T21’ relative to a ratio of 17:29 in dyad ‘A02’ suggests that Child ‘T21’ followed up on their parents’ vocalizations much more often than Child ‘A02’. Child ‘A02’ also interjected into their parent’s vocalizations more often than Child ‘T21’ did, as indicated by interruptive-to-switching turn frequency ratios.

Table 5. Descriptive Statistics of Vocal Turn Frequency and Duration Per Person

Vocal State	Frequency	Duration (sec)				
		M	SD	Mdn	IQR	[Min, Max]
‘A02’ Child						
Switching Turn	15	2.8	0.9	2.8	1.5	[1.0, 4.2]
Interruptive Turn	30	2.1	1.4	1.5	1.4	[0.8, 8.0]
‘A02’ Parent						
Switching Turn	17	3.3	1.2	3.3	2.3	[1.5, 5.5]
Interruptive Turn	29	1.7	3.3	2.5	1.5	[1.5, 8.8]
‘T21’ Child						
Switching Turn	46	3.1	2.1	2.8	1.7	[1.0, 11.5]
Interruptive Turn	11	3.5	4.4	1.8	1.4	[1.3, 17.0]
‘T21’ Parent						
Switching Turn	61	3.8	3.3	2.5	2.8	[1.0, 14.3]
Interruptive Turn	25	3.8	3.3	2.5	2.8	[1.0, 14.3]

4.3 Measuring Dyadic Synchrony

To date, I have implemented the following nonlinear time series techniques to measure trend, concurrent, and lagged synchrony in my pilot data: 1) dynamic time warping, 2) cross-recurrence quantification analysis, and 3) cross-wavelet analysis. Below, I present preliminary findings from exploratory analyses of the pilot data and their resulting synchrony measurements. Given the pilot data’s small sample size, no statistical significance testing of between-dyad differences was performed. Preliminary findings are contextualized with regards to parent-child trend,

concurrent, and lagged synchrony in relation to Supported and Coordinated JE events, as well as dyadic proximity where possible.

4.3.1 Descriptive Analyses

Descriptive statistics of parent and child HR and HRV RMSSD were computed across the entire 'Dyadic Play' task and separately during Supported and Coordinated JE periods. Overall, dyad 'A02' showed higher HR values (child: $M = 129.54$ bpm, $SD = 10.39$; parent: $M = 75.38$ bpm, $SD = 7.92$) than dyad 'T21' (child: $M = 107.61$ bpm, $SD = 7.28$; parent: $M = 68.69$ bpm, $SD = 6.77$) during the task. Child 'A02' showed smaller RMSSD values ($M = 12.23$ ms, $SD = 5.56$) than Child 'T21' ($M = 20.76$, $SD = 10.60$), and Parent 'A02' showed larger RMSSD values ($M = 59.95$, $SD = 26.78$) than Parent 'T21' ($M = 33.88$, $SD = 9.49$). During both Supported and Coordinated JE (Figure 7), Child 'A02' also showed smaller average and median RMSSD than Child 'T21', but greater variability in RMSSD during Supported than Coordinated JE. These trends contrast with those of Child 'T21', whose RMSSD variability was actually greater during Coordinated than Supported JE. Oppositely, Parent 'A02' exhibited larger average and median HRV RMSSD than Parent 'T21' during both Supported and Coordinated JE. Similar to their child, Parent 'A02' also had greater variability in HRV RMSSD during Supported than Coordinated JE.

4.3.2 Dynamic Time Warping

Dynamic time warping analysis was performed with the *FastDTW* Python package ([Salvador & Chan, 2007](#)) on parent and child HR, HRV RMSSD, and vocal turn-taking across the entire 'Dyadic Play' task. Given differences in HR magnitudes between adults and children ([Ostchega et al., 2011](#)), parent and child HR values were rescaled with min-max normalization prior to DTW. The Euclidean distance function was used to calculate the alignment cost of corresponding points between the time series of cardiac data. For categorical vocal turn-taking data, a custom distance function was used to assign costs based on dissimilarities between labels, with a cost of 0 for switching turns, 1 for interruptive turns, and 0.5 for any other combination of labels. Costs were set based on the rationale that switching turns reflect coordination of conversational turns, while interruptive turns may disrupt the flow of conversation. The distance function was then used to calculate the alignment cost by evaluating the global cost of the optimal warping path. Each alignment cost was subsequently normalized by dividing this global cost by the sum of the lengths of both time series.

In all measures, Dyad 'A02' showed greater alignment costs than Dyad 'T21', suggesting less trend synchrony in HR, HRV RMSSD, and vocal turn-taking. As shown by their more irregular and curved optimal warping paths in DTW plots

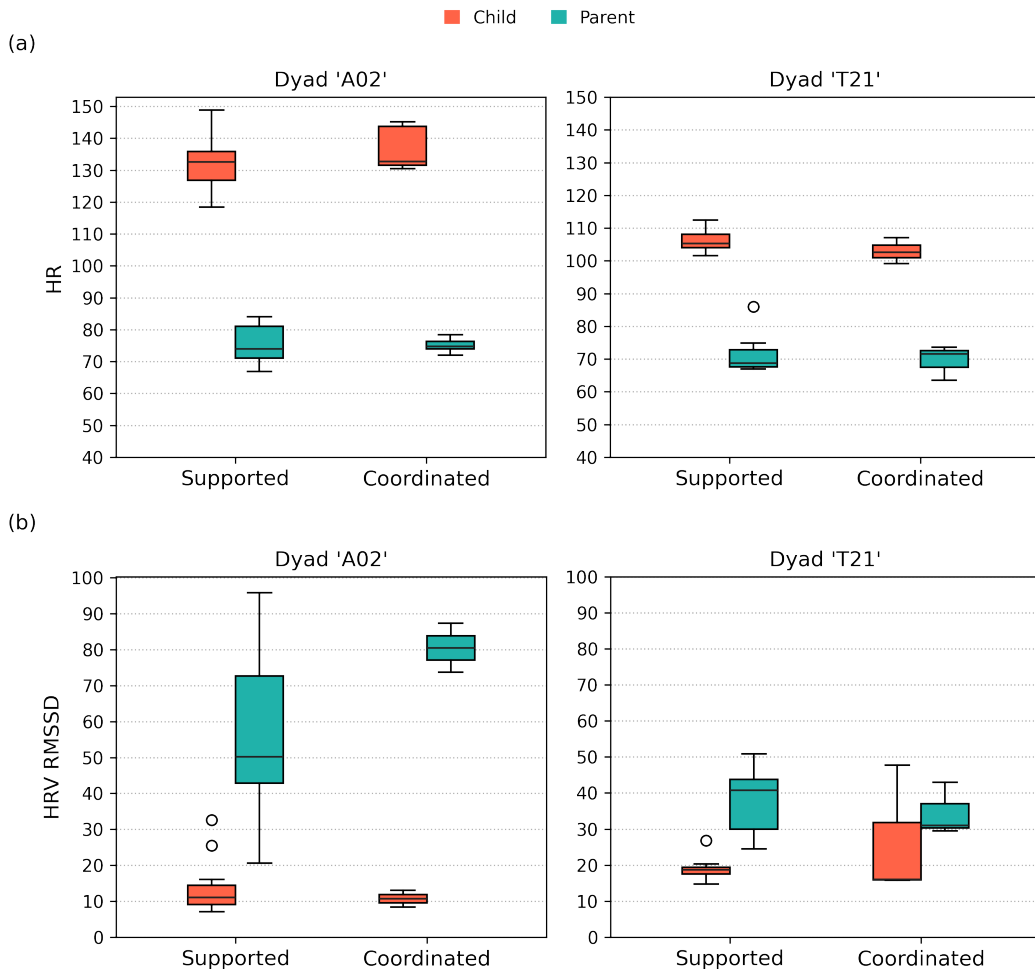


Figure 7. Distributions of (a) HR and (b) HRV RMSSD values by person and JE state.

(Figure 8), parent-child HRV RMSSD exhibited the least temporal alignment. In contrast, parent-child HR showed the greatest temporal alignment, as reflected by straighter and more diagonal warping paths. Similarly, DTW plots for parent-child vocal turn-taking (Figure 8c) also reflect relatively diagonal optimal warping paths, with a slightly greater alignment cost for dyad 'A02' than for dyad 'T21'.

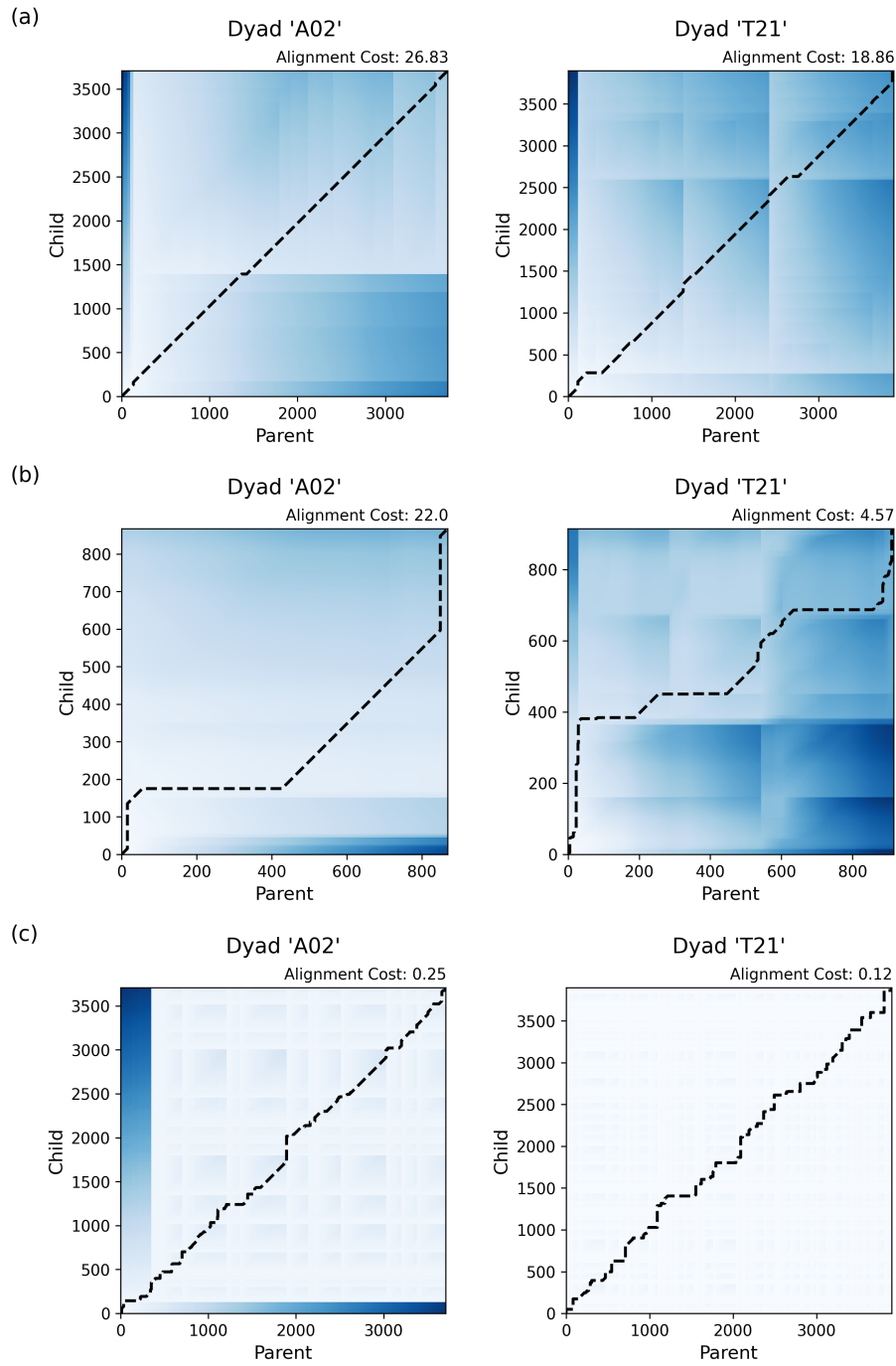


Figure 8. Dynamic time warping alignment plots of parent-child (a) HR, (b) HRV RMSSD, and (3) vocal turn-taking during ‘Dyadic Play’. Axis values represent number of samples per time series. Darker-shaded regions represent areas of higher alignment cost.

4.3.3 Cross-Recurrence Quantification Analysis

CRQA on parent-child HR and HRV RMSSD over the entire ‘Dyadic Play’ task was performed using the *PyRQA* Python package (Rawald, Sips, & Marwan, 2017). For each physiological data type, optimal embedding dimension (M), time delay (D), and fixed radius (r) values were evaluated using the false nearest neighbors (FNN) method, average mutual information (AMI), and recurrence rates, respectively. Optimal parameters must be selected to minimize the effects of autocorrelation, ensuring the most independent and accurate reconstruction of the system’s dynamics for CRQA. The FNN procedure identifies when points that appear to be neighbors in lower dimensions are no longer neighbors in higher dimensions, while average mutual information quantifies the amount of shared information between a time series and its delayed version. Thus, M and D values corresponding to their first local minima are chosen (Kantz & Schreiber, 1997; Marwan, 2011). Finally, optimal fixed radius values are those with resulting recurrence rates between 1% and 10% across all dyad members (Denk et al., 2024).

For both HR and HRV RMSSD, a range of 1 to 15 embedding dimensions was evaluated with FNN. In contrast, because of differences in the nature and sampling rates of the HR and HRV RMSSD data, different ranges of time delays between HR and RMSSD time series were used to calculate average mutual information. Accordingly, a range of time delays from 1 to 30 seconds was selected for HR time series, and a range from 1 to 60 seconds was selected for HRV RMSSD time series. For each parent and child time series, an optimal embedding dimension and time delay were found using the first local minimum of the FNN and AMI functions each, respectively. For FNN, if no local minimum was found, the first parameter value at which FNN values became stable (i.e., where consecutive differences between values fell below .001, indicating minimal changes) was used. Finally, a single optimal embedding dimension and time delay each for both dyads were calculated as the mean plus one standard deviation of all dyad members’ respective M and D values. The optimal embedding dimension was found to be 8, and the optimal time delays were 4 and 15 seconds for HR and HRV RMSSD, respectively (see Figure 1 in the Appendix). Using these M and D values, CRQA yielded recurrence rates closest to 10% at fixed radii values of 1.5 and 0.7 for HR and HRV RMSSD, respectively.

With the above parameters, CRQA was performed on parent-child HR and HRV RMSSD of pilot dyads. Recurrence rates, determinism, average and longest diagonal line lengths, and diagonal line entropy values for each dyad by data type are shown in Table 6.

Table 6. CRQA of Parent-Child Cardiac Time Series

Metric	HR		HRV RMSSD	
	Dyad 'A02'	Dyad 'T21'	Dyad 'A02'	Dyad 'T21'
RR, %	1.57	1.49	0.28	1.43
Det, %	91.32	91.04	86.97	94.21
L_{mean}	3.90	3.83	4.99	7.54
L_{max}	112	57	17	79
$L_{entropy}$	1.83	1.82	2.17	2.52

Note. RR = recurrence rate, Det = determinism, L_{mean} = mean diagonal line length, L_{max} = longest diagonal line length, $L_{entropy}$ = diagonal line entropy. Bolded numbers indicate greater measures between dyads.

HR and HRV RMSSD cross-recurrence plots show that dyads 'A02' and 'T21' exhibit similar levels of cardiac trend synchrony (refer to Figure 2 in the Appendix). With regards to HR, dyad 'A02' showed only marginally higher values than dyad 'T21' in all CRQA metrics except in longest diagonal line length. 'A02's longest diagonal line length was considerably greater than that of 'T21', suggesting longer and more stable periods of HR synchrony. While comparable, HR entropy outcomes also show that dyad 'A02' had slightly more varied and less predictable patterns of synchrony than dyad 'T21'. These outcomes may be related to the greater variability observed in child HR values in dyad 'A02' than in dyad 'T21' (Figure 7).

The opposite trend is observed in parent-child HRV RMSSD. In all CRQA metrics, dyad 'T21' exhibited higher values, suggesting greater frequency and durations of HRV synchrony than dyad 'A02'. Additionally, greater diagonal line entropy in dyad 'T21' suggests slightly greater diversity in durations of HRV synchrony, compared to that in dyad 'A02'. Overall, dyad 'T21's greater HRV RMSSD synchrony suggests a more flexible and adaptive dyadic play interaction involving mutual physiological regulation.

4.3.4 Cross-Wavelet Analysis

Cross-wavelet analysis of parent-child HR and HRV RMSSD was performed with the *pycwt* package (Krieger & Freij, 2023). For HR data sampled at 4 Hz, the analysis covered periods from 0.5 second to 32 seconds corresponding to frequencies of 2 Hz and 0.03 Hz, respectively. For HRV RMSSD data sampled at 1 Hz, analyzed periods ranged from 2 seconds (0.5 Hz) to 256 seconds (0.004 Hz). Overall, wavelet coherence plots (Figure 9) revealed no salient differences in HR synchrony between dyads 'A02' and 'T21' across time and frequency bands. In contrast, multiple episodes of high parent-child HRV RMSSD synchrony (i.e., coherence values of at least 0.7) emerged

in the low-frequency (LF; 6 to 25 seconds) and high-frequency (HF; 2 to 6 seconds) bands in both dyads.

Increased HRV RMSSD coherence in low- and high-frequency ranges can be interpreted as greater *trend* and *concurrent synchrony*, respectively (Denk et al., 2024). Given the emergence of high-coherence episodes in low- and high-frequency ranges, HRV RMSSD coherence values were further analyzed with respect to joint engagement type specifically within these ranges.

In LF ranges (Figure 10a), both dyads exhibited higher parent-child HRV RMSSD coherence during Coordinated JE compared to Supported JE. Dyad 'A02' also exhibited marginally higher LF HRV RMSSD coherence during both Supported and Coordinated JE compared to dyad 'T21'. However, dyad 'T21' displayed greater variability in LF coherence values during Coordinated JE than dyad 'A02'. Similarly,

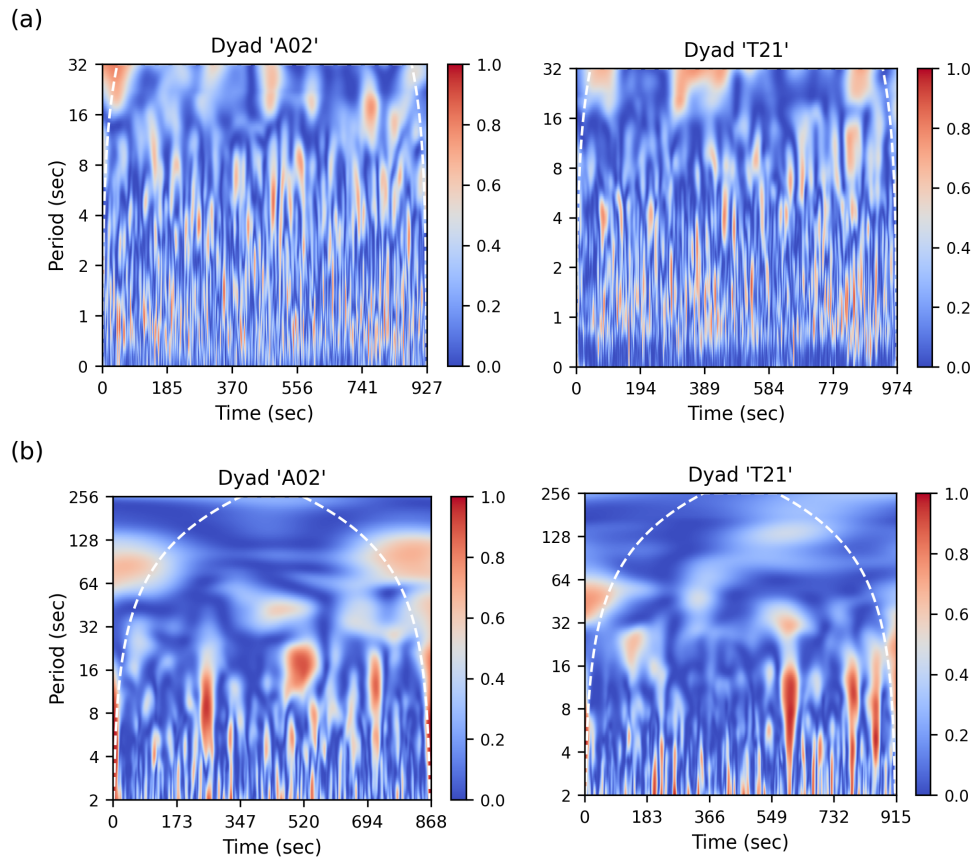


Figure 9. Continuous wavelet coherence plots of parent-child (a) HR and (b) HRV RMSSD values by dyad. Frequency bands are given in periods in seconds. White dashed lines demarcate the cone of influence in each dyad's time-frequency analysis.

in HF ranges (Figure 10b), dyad 'T21' demonstrated greater variability in HRV RMSSD coherence during Coordinated JE compared to dyad 'A02'. However, dyad 'T21's coherence during Coordinated JE was not noticeably higher than their coherence during Supported JE. Together, these results highlight that, during Supported JE, both dyads exhibited similar patterns of HRV RMSSD trend and concurrent synchrony. Further, during Coordinated JE, dyad 'T21' exhibited wide ranges of HRV RMSSD trend and concurrent synchrony, while dyad 'A02' exhibited smaller ranges, with coherence values below 0.7.

Given that cross-wavelet analysis can capture synchrony with temporal resolution, I also assessed correlations between parent-child coherence and dyadic proximity. Spearman's rank correlation tests revealed weak correlations between parent-child HRV RMSSD coherence values and dyadic proximity in both dyads (Figure 11). To address the issue of missing dyadic proximity values, dyadic proximity and HRV RMSSD coherence time series were each mean-aggregated over 5-second windows before calculating correlations. In dyad 'A02', LF and HF HRV RMSSD coherence values showed weak and statistically insignificant correlations with dyadic

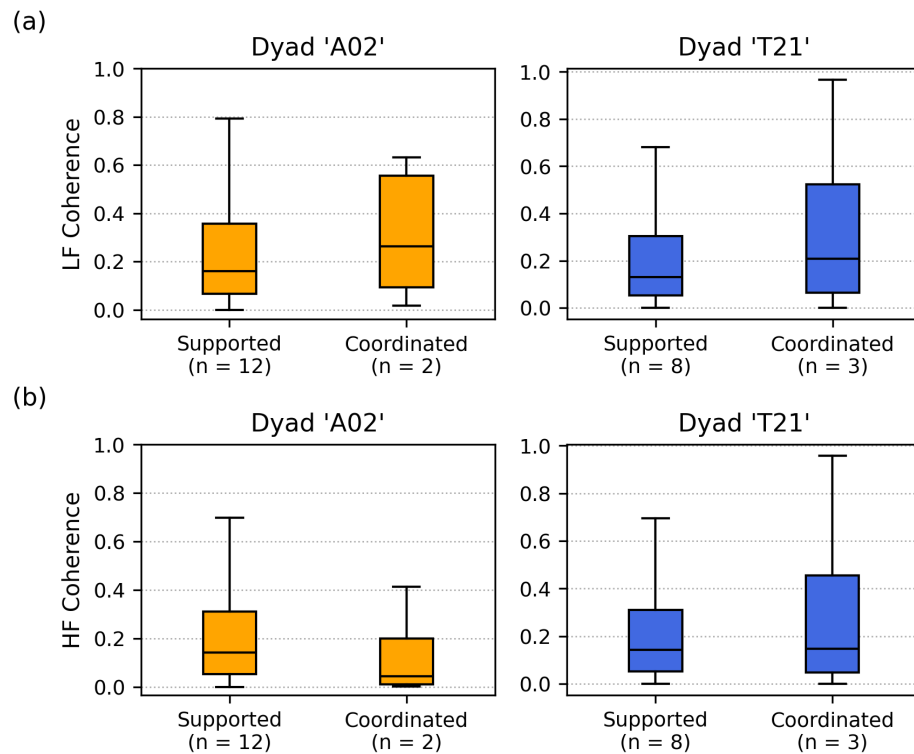


Figure 10. Distributions of (a) low-frequency and (b) high-frequency HRV RMSSD coherence by dyad and JE state.

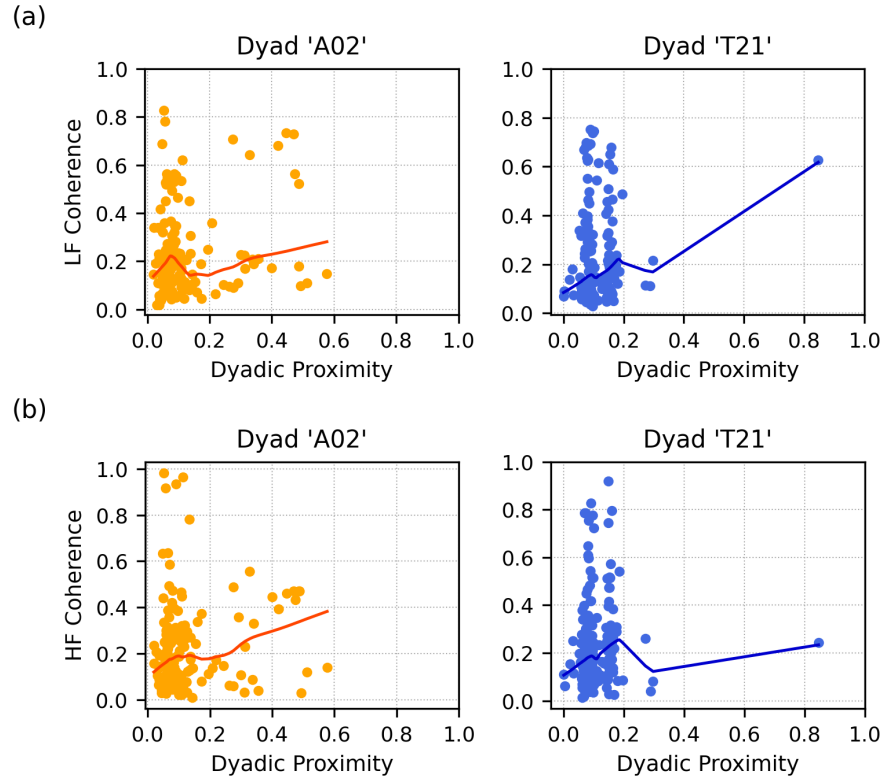


Figure 11. Scatterplots of (a) low-frequency and (b) high-frequency HRV RMSSD coherence by dyad. Lines represent locally weighted/estimated scatterplot smoothing curves.

proximity (LF: $\rho = 0.02$, $p = 0.81$; HF: $\rho = 0.15$, $p = 0.07$). Conversely, in dyad 'T21', correlation coefficients between LF and HF HRV RMSSD coherence and dyadic proximity were small but significant (LF: $\rho = 0.18$, $p = 0.02$; HF: $\rho = 0.17$, $p = 0.02$). Altogether, these results highlight that parent-child HRV RMSSD trend and concurrent synchrony are not strongly influenced by physical closeness in these dyads.

To investigate lagged HR and HRV RMSSD synchrony, I examined the phase angle differences corresponding to time-frequency points of high synchrony (i.e., coherence values of at least 0.7) throughout the entire 'Dyadic Play' task and during Supported and Coordinated JE. Table 7 display proportions of time HR and HRV RMSSD values of each parent and child spent leading synchrony changes. Overall, both children's HR led the majority of the time, with the exception of Child 'A02's HR during Coordinated JE. For HRV RMSSD, proportions of time spent leading and following were comparable across dyad members, regardless of whether the dyad participated in Supported or Coordinated JE.

Table 7. Proportions of Time Leading and Following in High Cardiac Synchrony

Dyad	HR			HRV RMSSD		
	Entire	Supported	Coordinated	Entire	Supported	Coordinated
'A02'						
Child	62.6	62.2	33.7	51.4	53.2	--
Parent	37.4	37.8	66.3	48.6	46.8	--
'T21'						
Child	80.6	80.3	93.4	48.9	47.1	57.8
Parent	19.4	19.7	6.6	51.1	52.9	42.2

Note. No high coherence values were observed during Coordinated JE events in dyad 'A02'. Bolded numbers indicate greater measures between dyad members.

4.4 Key Findings and Considerations for Next Steps

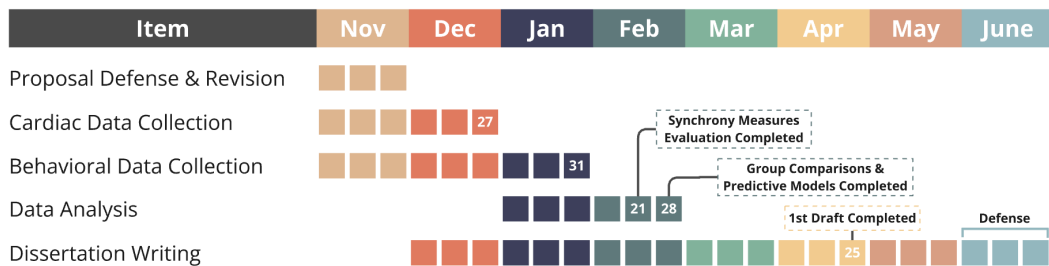
My work to date has focused on gaining clarity on the data quality and feasibility of obtaining continuous measures of interest from the enTRAIN dataset. Overall, ECG recordings of dyads with ASD contain more noise than those of TD dyads, with averages of 14.6% missing and 44% artifactual beats per segment in the ASD group and 5.5% missing and 40.9% artifactual beats per segment in the TD group. Given these quality assessment results, I will set criteria for usable ECG data with flexibility, allowing no more than 30% missing beats per segment and no more than 60% artifactual beats per segment on average. For all ECG recordings that do not meet criteria for usability, I will perform a more thorough quality assessment using a sliding window approach to inspect the data continuously and maximize the amount of usable ECG data from each recording. Lastly, each ECG segment will undergo a combination of automated and manual beat correction steps with PhysioView. For each correction procedure, the average proportion of beats corrected in each segment will be recorded.

My feasibility work and preliminary calculations of synchrony on pilot data have highlighted two issues to consider. First, DTW and CRQA require a minimum amount of data to yield interpretable results (Brick et al., 2018), but behavioral events such as vocal turns and joint engagement states may be only a few minutes long. Therefore, increasing temporal resolution via windowing or computing alignment as well as generating cross-recurrence plots for physiological and behavioral data during specific joint engagement events, may be unfeasible. Dyad-level aggregation of proximity, as well as frequencies and durations of vocal turns and joint engagement states may be required for analysis with DTW and CRQA metrics.

Second, determining the optimal distance function for categorical vocal turn-taking data in DTW and CRQA remains uncertain (Hermann et al., 2023; Wallot et al., 2018). Unlike continuous data, for which well-established distance functions such as Euclidean distance can be applied, categorical data may present challenges when defining meaningful distances between states. Therefore, it may be necessary to further test and optimize the custom distance function used in DTW and CRQA of vocal turn-taking data.

For each synchrony measure, spurious results can occur when apparent patterns arise due to random chance or signal properties that are unrelated to true synchrony. In linear methods such as cross-correlations, for example, correlation coefficients can be affected by autocorrelation, where time series correlate with their own past values. To control for this, I will apply prewhitening to the time series before computing cross-correlations. Additionally, I will conduct surrogate testing (Ramseyer & Tschacher, 2010), also referred to as bootstrapping or permutation testing. In this approach, time series from different dyad members are randomly paired to form a new, artificial set of dyadic data on which synchrony is recalculated. For each measure, I will then use t-tests to compare the synchrony results of the original set with those of the artificial set. This procedure will reveal whether the observed patterns in the original set of dyads are statistically significant or simply random coincidences.

5. Proposed Timeline



References

- Adamson, L. B., Bakeman, R., & Deckner, D. F. (2004). The development of symbol-infused joint engagement. *Child Development*, 75(4), 1171–1187. <https://doi.org/10.1111/j.1467-8624.2004.00732.x>
- American Psychiatric Association. (2013). *Diagnostic and statistical manual of mental disorders* (5th ed.). <https://doi.org/10.1176/appi.books.9780890425596>
- Bajpai, R., & Joshi, D. (2021). MoveNet: A deep neural network for joint profile prediction across variable walking speeds and slopes. *IEEE Transactions on Instrumentation and Measurement*, 70, 1–11. <https://doi.org/10.1109/TIM.2021.3073720>
- Bakeman, R., & Adamson, L. B. (1984). Coordinating attention to people and objects in mother-infant and peer-infant interaction. *Child Development*, 55(4), 1278–1289. <https://doi.org/10.2307/1129997>
- Baker, J. K., Fenning, R. M., Howland, M. A., Baucom, B. R., Moffitt, J., & Erath, S. A. (2015). Brief report: A pilot study of parent-child biobehavioral synchrony in autism spectrum disorder. *Journal of Autism and Developmental Disorders*, 45(12), 4140–4146. <https://doi.org/10.1007/s10803-015-2528-0>
- Bernieri, F. J., & Rosenthal, R. (1991). Interpersonal coordination: Behavior matching and interactional synchrony. In R. S. Feldman & B. Rime (Eds.), *Fundamentals of nonverbal behavior* (pp. 401–432). Cambridge University Press.
- Berntson, G. G., Quigley, K. S., Jang, J. F., & Boysen, S. T. (1990). An approach to artifact identification: Application to heart period data. *Psychophysiology*, 27(5), 586–598. <https://doi.org/10.1111/j.1469-8986.1990.tb01982.x>
- Brick, T. R., Gray, A. L., & Staples, A. D. (2018). Recurrence quantification for the analysis of coupled processes in aging. *The Journals of Gerontology: Series B*, 73(1), 134–147. <https://doi.org/10.1093/geronb/gbx018>
- Budman, I., Meiri, G., Ilan, M., Faroy, M., Langer, A., Reboh, D., Michaelovski, A., Flusser, H., Menashe, I., Donchin, O., & Dinstein, I. (2019). Quantifying the social symptoms of autism using motion capture. *Scientific Reports*, 9(1), 1–8. <https://doi.org/10.1038/s41598-019-44180-9>
- Capraz, Y. Z., Konrad, K., & Reindl, V. (2023). Concurrent and lagged physiological synchrony during mother-child interaction and their relationship to positive affect in 8- to 10-year-old children. *Scientific Reports*, 13(1), 1–13. <https://doi.org/10.1038/s41598-023-43847-8>
- Carnevali, L., Valori, I., Mason, G., Altoè, G., & Farroni, T. (2024). Interpersonal motor synchrony in autism: A systematic review and meta-analysis. *Frontiers in Psychiatry*, 15, 1–20. <https://doi.org/10.3389/fpsyg.2024.1355068>
- Chatel-Goldman, J., Congedo, M., Jutten, C., & Schwartz, J.-L. (2014). Touch increases autonomic coupling between romantic partners. *Frontiers in Behavioral Neuroscience*, 8, 1–12. <https://doi.org/10.3389/fnbeh.2014.00095>
- Chen, X., Chen, J., Liao, M., & Wang, G. (2023). Early onset of impairments of interpersonal motor synchrony in preschool-aged children with autism spectrum disorder. *Journal of Autism and Developmental Disorders*, 53(6), 2314–2327. <https://doi.org/10.1007/s10803-022-05472-8>

- Cohn, J. F., & Tronick, E. Z. (1987). Mother-infant face-to-face interaction: The sequence of dyadic states at 3, 6, and 9 months. *Developmental Psychology*, 23(1), 68–77.
<https://doi.org/10.1037/0012-1649.23.1.68>
- Constantino, J. N., & Gruber, C. P. (2012). *Social Responsiveness Scale, Second Edition (SRS-2)*. Western Psychological Services.
- Dataavyu Team. (2014). Dataavyu: A video coding tool. Databrary Project, New York University.
<http://dataavyu.org>
- Dettori, J. R., & Norvell, D. C. (2020). Kappa and beyond: Is there agreement? *Global Spine Journal*, 10(4), 499–501. <https://doi.org/10.1177/2192568220911648>
- Denk, B., Dimitroff, S., Meier, M., Wienhold, S., Gaertner, R., Klink, E. S. C., Benz, A., Bentele, U. U., & Pruessner, J. C. (2024). Physiological synchrony of the autonomic nervous system—An analysis and comparison of different methods. OSF PsyArXiv.
<https://doi.org/10.31234/osf.io/dws8c>
- DePasquale, C. E. (2021). A systematic review of caregiver-child physiological synchrony across systems: Associations with behavior and child functioning. *Development and Psychopathology*, 32(5), 1754–1777. <https://doi.org/10.1017/S0954579420001236>
- Dunsmore, J. C., Ashley, R. A., Zhou, Y., Swain, D. M., Factor, R. S., Broomell, A. P., Waldron, J. C., Bell, M. A., & Scarpa, A. (2019). Marching to the beat of your own drum?: A proof-of-concept study assessing physiological linkage in autism spectrum disorder. *Biological Psychology*, 144, 37–45. <https://doi.org/10.1016/j.biopsych.2019.03.001>
- Duong, S., Davis, T., Bachman, H., Votruba-Drzal, E., & Libertus, M. (2024). Dynamic structures of parent-child number talk: An application of categorical cross-recurrence quantification analysis and companion to Duong et al. (2024). *The Quantitative Methods for Psychology*, 20, 137–155. <https://doi.org/10.20982/tqmp.20.2.p137>
- Feldman, R. (2007). Parent-infant synchrony: Biological foundations and developmental outcomes. *Current Directions in Psychological Science*, 16(6), 340–345.
<https://doi.org/10.1111/j.1467-8721.2007.00532.x>
- Feldman, R., Magori-Cohen, R., Galili, G., Singer, M., & Louzoun, Y. (2011). Mother and infant coordinate heart rhythms through episodes of interaction synchrony. *Infant Behavior and Development*, 34(4), 569–577. <https://doi.org/10.1016/j.infbeh.2011.06.008>
- Fitzpatrick, P., Frazier, J. A., Cochran, D. M., Mitchell, T., Coleman, C., & Schmidt, R. C. (2016). Impairments of social motor synchrony evident in autism spectrum disorder. *Frontiers in Psychology*, 7, 1323. <https://doi.org/10.3389/fpsyg.2016.01323>
- Föll, S., Maritsch, M., Spinola, F., Mishra, V., Barata, F., Kowatsch, T., ... & Wortmann, F. (2021). FLIRT: A feature generation toolkit for wearable data. *Computer Methods and Programs in Biomedicine*, 212, 106461. <https://doi.org/10.1016/j.cmpb.2021.106461>
- Freeman, S., & Kasari, C. (2013). Parent-child interactions in autism: Characteristics of play. *Autism*, 17(2), 147–161. <https://doi.org/10.1177/1362361312469269>
- Graham, F. K. (1978). Constraints on measuring heart rate and period sequentially through real and cardiac time. *Psychophysiology*, 15(5), 492–495. <https://doi.org/10.1111/j.1469-8986.1978.tb01422.x>

- Gessaroli, E., Santelli, E., di Pellegrino, G., & Frassinetti, F. (2013). Personal space regulation in childhood autism spectrum disorders. *PLoS ONE*, 8(9), Article e74959, 1–8. <https://doi.org/10.1371/journal.pone.0074959>
- Georgescu, A. L., Koeroglu, S., Hamilton, A. F. D. C., Vogeley, K., Falter-Wagner, C. M., & Tschacher, W. (2020). Reduced nonverbal interpersonal synchrony in autism spectrum disorder independent of partner diagnosis: A motion energy study. *Molecular Autism*, 11, 1–14. <https://doi.org/10.1186/s13229-019-0305-1>
- Glass, D., & Yuill, N. (2023). Social motor synchrony in autism spectrum conditions: A systematic review. *Autism*, 28(7), 1638–1653. <https://doi.org/10.1177/13623613231213295>
- Glass, D., & Yuill, N. (2024). Moving together: Social motor synchrony in autistic peer partners depends on partner and activity type. *Journal of Autism and Developmental Disorders*, 54(8), 2874–2890. <https://doi.org/10.1007/s10803-023-05917-8>
- Griffioen, R. E., van der Steen, S., Verheggen, T., Enders-Slegers, M.-J., & Cox, R. (2020). Changes in behavioural synchrony during dog-assisted therapy for children with autism spectrum disorder and children with Down syndrome. *Journal of Applied Research in Intellectual Disabilities*, 33(3), 398–408. <https://doi.org/10.1111/jar.12682>
- Grinsted, A., Moore, J. C., & Jevrejeva, S. (2004). Application of the cross wavelet transform and wavelet coherence to geophysical time series. *Nonlinear Processes in Geophysics*, 11(5/6), 561–566. <https://doi.org/10.5194/npg-11-561-2004>
- Gwet, K. L. (2008). Computing inter-rater reliability and its variance in the presence of high agreement. *The British Journal of Mathematical and Statistical Psychology*, 61(1), 29–48. <https://doi.org/10.1348/000711006X126600>
- Hartley, R., & Zisserman, A. (2004). Multiple view geometry in computer vision (2nd ed.). Cambridge University Press. <https://doi.org/10.1017/CBO9780511811685>
- Hegarty-Craver, M., Gilchrist, K. H., Propper, C. B., Lewis, G. F., DeFilipp, S. J., Coffman, J. L., & Willoughby, M. T. (2018). Automated respiratory sinus arrhythmia measurement: Demonstration using executive function assessment. *Behavior Research Methods*, 50(5), 1816–1823. <https://doi.org/10.3758/s13428-017-0950-2>
- Helm, J. L., Miller, J. G., Kahle, S., Troxel, N. R., & Hastings, P. D. (2018). On measuring and modeling physiological synchrony in dyads. *Multivariate Behavioral Research*, 53(4), 521–543. <https://doi.org/10.1080/00273171.2018.1459292>
- Herrmann, M., Tan, C. W., & Webb, G. I. (2023). Parameterizing the cost function of dynamic time warping with application to time series classification. *Data Mining and Knowledge Discovery*, 37(5), 2024–2045. <https://doi.org/10.1007/s10618-023-00926-8>
- Hilty, M., Oldrati, P., Barrios, L., Müller, T., Blumer, C., Foege, M., PHRT Consortium, Holz, C., & Lutterotti, A. (2022). Continuous monitoring with wearables in multiple sclerosis reveals an association of cardiac autonomic dysfunction with disease severity. *Multiple Sclerosis Journal—Experimental, Translational and Clinical*, 8(2), 1–12. <https://doi.org/10.1177/20552173221103436>
- Hobson, R. P., Hobson, J. A., García-Pérez, R., & Du Bois, J. (2012). Dialogic linkage and resonance in autism. *Journal of Autism and Developmental Disorders*, 42(12), 2718–2728. <https://doi.org/10.1007/s10803-012-1528-6>

- Hoemann, K., Khan, Z., Feldman, M. J., Nielson, C., Devlin, M., Dy, J., Barrett, L. F., Wormwood, J. B., & Quigley, K. S. (2020). Context-aware experience sampling reveals the scale of variation in affective experience. *Scientific Reports*, 10(1), 1–16. <https://doi.org/10.1038/s41598-020-69180-y>
- Jaffe, J., & Feldstein, S. (1970). Rhythms of dialogue. Academic Press.
- Jaffe, J., Beebe, B., Feldstein, S., Crown, C. L., Jasnow, M. D., Rochat, P., & Stern, D. N. (2001). Rhythms of dialogue in infancy: Coordinated timing in development. *Monographs of the Society for Research in Child Development*, 66(2), i–149. <https://pubmed.ncbi.nlm.nih.gov/11428150/>
- Kantz, H., & Schreiber, T. (1997). *Nonlinear time series analysis*. Cambridge University Press.
- Krieger, S., & Freij, N. (2023). *PyCWT: Wavelet spectral analysis in Python* (Version 0.4.0-beta) [Software]. <https://github.com/regeirk/pycwt>
- Kristiansen, J., Korshøj, M., Skotte, J. H., Jespersen, T., Søgaard, K., Mortensen, O. S., & Holtermann, A. (2011). Comparison of two systems for long-term heart rate variability monitoring in free-living conditions: A pilot study. *BioMedical Engineering OnLine*, 10(1), 1–14. <https://doi.org/10.1186%2F1475-925X-10-27>
- Lampi, A., Fitzpatrick, P., Romero, V., Amaral, J., & Schmidt, R. C. (2020). Understanding the influence of social and motor context on the co-occurring frequency of restricted and repetitive behaviors in autism. *Journal of Autism and Developmental Disorders*, 50(5), 1479–1496. <https://doi.org/10.1007/s10803-018-3698-3>
- Levenson, R. W. (2024). Two's company: Biobehavioral research with dyads. *Biological Psychology*, 185, 1–7. <https://doi.org/10.1016/j.biopsych.2023.108719>
- Lin, T.-Y., Maire, M., Belongie, S., Hays, J., Perona, P., Ramanan, D., Dollár, P., & Zitnick, C. L. (2014). Microsoft COCO: Common Objects in Context. In D. Fleet, T. Pajdla, B. Schiele, & T. Tuytelaars (Eds.), *Computer Vision – ECCV 2014* (pp. 740–755). Springer International Publishing. https://doi.org/10.1007/978-3-319-10602-1_48
- López Pérez, D., Leonardi, G., Niedźwiecka, A., Radkowska, A., Rączaszek-Leonardi, J., & Tomalski, P. (2017). Combining recurrence analysis and automatic movement extraction from video recordings to study behavioral coupling in face-to-face parent-child interactions. *Frontiers in Psychology*, 8, Article 2228, 1–14. <https://doi.org/10.3389/fpsyg.2017.02228>
- Louwerse, M. M., Dale, R., Bard, E. G., & Jeuniaux, P. (2012). Behavior matching in multimodal communication is synchronized. *Cognitive Science*, 36(8), 1404–1426. <https://doi.org/10.1111/j.1551-6709.2012.01269.x>
- Macdonald, R. G., & Tatler, B. W. (2018). Gaze in a real-world social interaction: A dual eye-tracking study. *Quarterly Journal of Experimental Psychology* (2006), 71(10), 2162–2173. <https://doi.org/10.1177/1747021817739221>
- Maenner, M. J., Warren, Z., Williams, A. R., Amoakohene, E., Bakian, A. V., Bilder, D. A., Durkin, M. S., Fitzgerald, R. T., Furnier, S. M., Hughes, M. M., Ladd-Acosta, C. M., McArthur, D., Pas, E. T., Salinas, A., Vehorn, A., Williams, S., Esler, A., Grzybowski, A., Hall-Lande, J., ... Shaw, K. A. (2023). Prevalence and characteristics of autism spectrum disorder among children aged 8 years—Autism and developmental disabilities

- monitoring network, 11 sites, United States, 2020. *MMWR Surveillance Summaries*, 72(2), 1–14. <https://doi.org/10.15585/mmwr.ss7202a1>
- Marsh, K. L., Isenhower, R. W., Richardson, M. J., Helt, M., Verbalis, A. D., Schmidt, R. C., & Fein, D. (2013). Autism and social disconnection in interpersonal rocking. *Frontiers in Integrative Neuroscience*, 7, 1–8. <https://doi.org/10.3389/fnint.2013.00004>
- Marwan, N., Wessel, N., Meyerfeldt, U., Schirdewan, A., & Kurths, J. (2002). Recurrence-plot-based measures of complexity and their application to heart-rate-variability data. *Physical Review E: Statistical, Nonlinear, and Soft Matter Physics*, 66(2 Pt 2), 026702. <https://doi.org/10.1103/PhysRevE.66.026702>
- Mayo, O., & Gordon, I. (2020). In and out of synchrony—Behavioral and physiological dynamics of dyadic interpersonal coordination. *Psychophysiology*, 57(6), e13574. <https://doi.org/10.1111/psyp.13574>
- McHugh, M. L. (2012). Interrater reliability: The kappa statistic. *Biochemia Medica*, 22(3), 276–282.
- McNaughton, K. A., & Redcay, E. (2020). Interpersonal synchrony in autism. *Current Psychiatry Reports*, 22(3), Article 12, 1–11. <https://doi.org/10.1007/s11920-020-1135-8>
- Menghini, L., Gianfranchi, E., Cellini, N., Patron, E., Tagliabue, M., & Sarlo, M. (2019). Stressing the accuracy: Wrist-worn wearable sensor validation over different conditions. *Psychophysiology*, 56(11), 1–15. <https://doi.org/10.1111/psyp.13441>
- Miller, J. G., Armstrong-Carter, E., Balter, L., & Lorah, J. (2022). A meta-analysis of mother-child synchrony in respiratory sinus arrhythmia and contextual risk. *Developmental Psychobiology*, 65(1), e22355. <https://doi.org/10.1002/dev.22355>
- Murat Baldwin, M., Xiao, Z., & Murray, A. (2022). Temporal synchrony in autism: A systematic review. *Review Journal of Autism and Developmental Disorders*, 9(4), 596–617. <https://doi.org/10.1007/s40489-021-00276-5>
- Ochi, K., Ono, N., Owada, K., Kojima, M., Kuroda, M., Sagayama, S., & Yamasue, H. (2019). Quantification of speech and synchrony in the conversation of adults with autism spectrum disorder. *PLOS ONE*, 14(12), 1–22. <https://doi.org/10.1371/journal.pone.0225377>
- Ostchega, Y., Porter, K. S., Hughes, J., Dillon, C. F., & Nwankwo, T. (2011). *Resting pulse rate reference data for children, adolescents, and adults; United States, 1999–2008* (No. 41). U.S. Department of Health and Human Services, Centers for Disease Control and Prevention, National Center for Health Statistics.
- Palumbo, R. V., Marraccini, M. E., Weyandt, L. L., Wilder-Smith, O., Liu, S., & Goodwin, M. S. (2016). Interpersonal autonomic physiology: A systematic review of the literature. *Personality and Social Psychology Review*, 21(2), 99–141. <https://doi.org/10.1177/1088868316628405>
- Patterson, S. Y., Elder, L., Gulsrud, A., & Kasari, C. (2014). The association between parental interaction style and children's joint engagement in families with toddlers with autism. *Autism: The International Journal of Research and Practice*, 18(5), 511–518. <https://doi.org/10.1177/1362361313483595>
- Plank, I. S., Traiger, L. S., Nelson, A. M., Koehler, J. C., Lang, S. F., Tepes, R., Vogeley, K., Georgescu, A. L., & Falter-Wagner, C. M. (2023). The role of interpersonal synchrony in forming impressions of autistic and non-autistic adults. *Scientific Reports*, 13(1), 1–12. <https://doi.org/10.1038/s41598-023-42006-3>

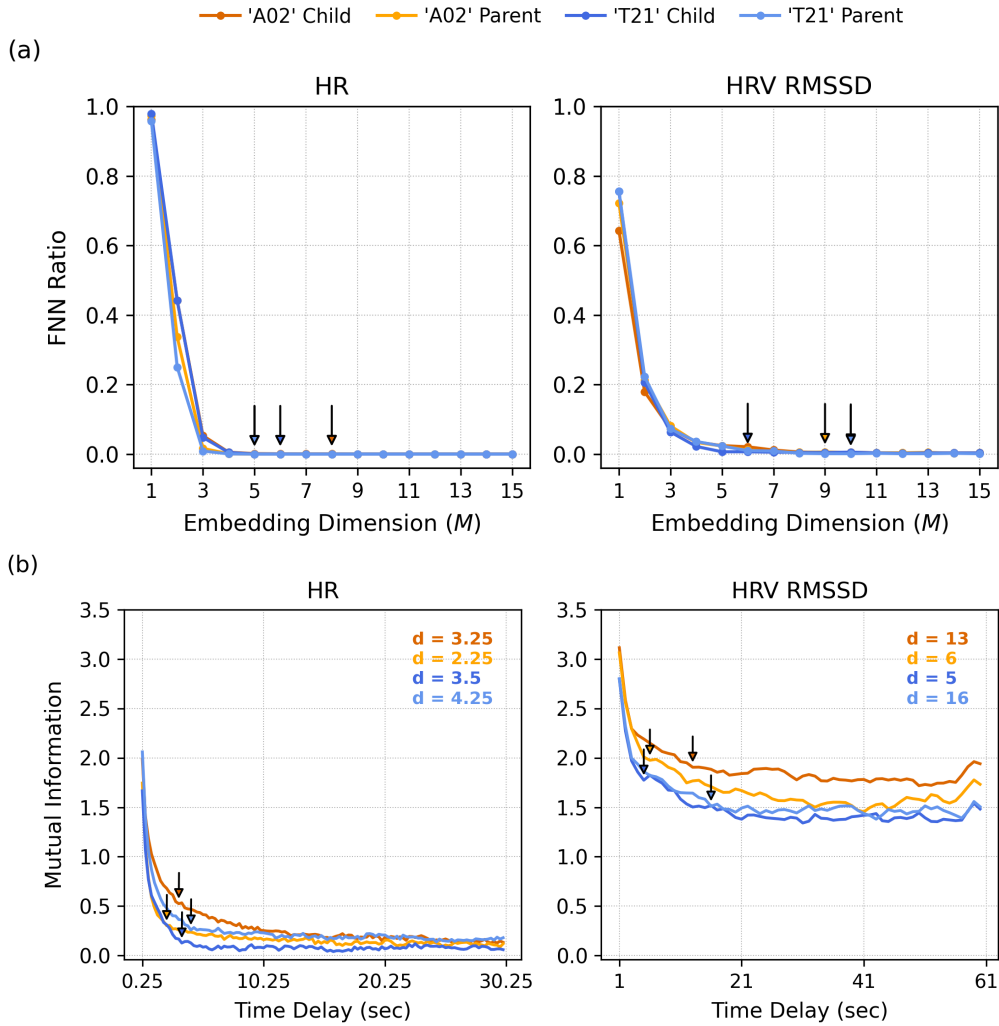
- Poh, M.-Z., Swenson, N. C., & Picard, R. W. (2010). A wearable sensor for unobtrusive, long-term assessment of electrodermal activity. *IEEE Transactions on Biomedical Engineering*, 57(5), 1243–1252. <https://doi.org/10.1109/TBME.2009.2038487>
- Ramseyer, F., & Tschacher, W. (2010). Nonverbal synchrony or random coincidence? How to tell the difference. In A. Esposito, N. Campbell, C. Vogel, A. Hussain, & A. Nijholt (Eds.), *Development of Multimodal Interfaces: Active Listening and Synchrony: Second COST 2102 International Training School, Dublin, Ireland, March 23-27, 2009, Revised Selected Papers* (pp. 182–196). Springer. https://doi.org/10.1007/978-3-642-12397-9_15
- Ranftl, R., Lasinger, K., Hafner, D., Schindler, K., & Koltun, V. (2020). Towards robust monocular depth estimation: Mixing datasets for zero-shot cross-dataset transfer. *arXiv*. <https://doi.org/10.48550/arXiv.1907.01341>
- Rawald, T., Sips, M., & Marwan, N. (2017). PyRQA—Conducting recurrence quantification analysis on very long time series efficiently. *Computers & Geosciences*, 104, 101–108. <https://doi.org/10.1016/j.cageo.2016.11.016>
- Reindl, V., Wass, S., Leong, V., Scharke, W., Wistuba, S., Wirth, C. L., Konrad, K., & Gerloff, C. (2022). Multimodal hyperscanning reveals that synchrony of body and mind are distinct in mother-child dyads. *NeuroImage*, 251, 118982. <https://doi.org/10.1016/j.neuroimage.2022.118982>
- Rennung, M., & Göritz, A. S. (2016). Prosocial consequences of interpersonal synchrony: A meta-analysis. *Zeitschrift Fur Psychologie*, 224(3), 168–189. <https://doi.org/10.1027/2151-2604/a000252>
- Richardson, M. J., Marsh, K. L., Isenhower, R. W., Goodman, J. R. L., & Schmidt, R. C. (2007). Rocking together: Dynamics of intentional and unintentional interpersonal coordination. *Human Movement Science*, 26(6), 867–891. <https://doi.org/10.1016/j.humov.2007.07.002>
- Salvador, S., & Chan, P. (2007). Toward accurate dynamic time warping in linear time and space. *Intelligent Data Analysis*, 11(5), 561–580. <https://doi.org/10.3233/IDA-2007-11508>
- Saunders Wilder, O., Sullivan, J., Johnson, K. T., Palumbo, R. V., Cumpanasiou, C., Picard, R. W., & Goodwin, M. S. (2018, May). Dyadic physiological interdependence and social reciprocity in ASD. *International Society for Autism Research (INSAR) Conference*, Rotterdam, Netherlands.
- Schmidt, P., Reiss, A., Duerichen, R., Marberger, C., & Van Laerhoven, K. (2018, October). Introducing WESAD, a multimodal dataset for wearable stress and affect detection. In Proceedings of the 20th ACM international conference on multimodal interaction (pp. 400-408). <https://doi.org/10.1145/3242969.3242985>
- Shaffer, F., & Ginsberg, J. P. (2017). An overview of heart rate variability metrics and norms. *Frontiers in Public Health*, 5, Article 258, 1–17. <https://doi.org/10.3389/fpubh.2017.00258>
- Stern, D., Jaffe, J., Beebe, B., & Bennett, S. (1975). Vocalizing in unison and in alternation. Two modes of communication within the mother-infant dyad. *Annals of the New York Academy of Sciences*, 263, 89–100. <https://doi.org/10.1111/j.1749-6632.1975.tb41574.x>

- Torrence, C., & Compo, G. P. (1998). A practical guide to wavelet analysis. *Bulletin of the American Meteorological Society*, 79(1), 61–78. [https://doi.org/10.1175/1520-0477\(1998\)079<0061:APGTWA>2.0.CO;2](https://doi.org/10.1175/1520-0477(1998)079<0061:APGTWA>2.0.CO;2)
- Tronick, E. Z., & Cohn, J. F. (1989). Infant-mother face-to-face interaction: Age and gender differences in coordination and the occurrence of miscoordination. *Child Development*, 60(1), 85–92. <https://doi.org/10.2307/1131074>
- Vintsyuk, T. K. (1968). Speech discrimination by dynamic programming. *Cybernetics*, 4(1), 52–57. <https://doi.org/10.1007/BF01074755>
- Wadge, H., Brewer, R., Bird, G., Toni, I., & Stolk, A. (2019). Communicative misalignment in autism spectrum disorder. *Cortex*, 115, 15–26. <https://doi.org/10.1016/j.cortex.2019.01.003>
- Wallot, S., & Leonardi, G. (2018). Analyzing multivariate dynamics using cross-recurrence quantification analysis (CRQA), diagonal-cross-recurrence profiles (DCRP), and multidimensional recurrence quantification analysis (MdRQA)—A tutorial in R. *Frontiers in Psychology*, 9. <https://doi.org/10.3389/fpsyg.2018.02232>
- Wang, H., Suveg, C., West, K. B., Han, Z. R., Zhang, X., Hu, X., & Yi, L. (2021). Synchrony of respiratory sinus arrhythmia in parents and children with autism spectrum disorder: Moderation by interaction quality and child behavior problems. *Autism Research*, 14(3), 512–522. <https://doi.org/10.1002/aur.2401>
- Yamane, N., Mishra, V., & Goodwin, M. S. (2024). HeartView: An extensible, open-source, web-based signal quality assessment pipeline for ambulatory cardiovascular data. In D. Salvi, P. Van Gorp, & S. A. Shah (Eds.), *Pervasive Computing Technologies for Healthcare* (pp. 107–123). Springer Nature Switzerland. https://doi.org/10.1007/978-3-031-59717-6_8
- Yoo, G. E., & Kim, S. J. (2018). Dyadic drum playing and social skills: Implications for rhythm-mediated intervention for children with autism spectrum disorder. *Journal of Music Therapy*, 55(3), 340–375. <https://doi.org/10.1093/jmt/thy013>
- Zbilut, J. P., & Webber, C. L. (1992). Embeddings and delays as derived from quantification of recurrence plots. *Physics Letters A*, 171(3), 199–203. [https://doi.org/10.1016/0375-9601\(92\)90426-M](https://doi.org/10.1016/0375-9601(92)90426-M)

Appendix

Figure 1

Evaluation results of optimal CRQA parameters using false nearest neighbors and average mutual information

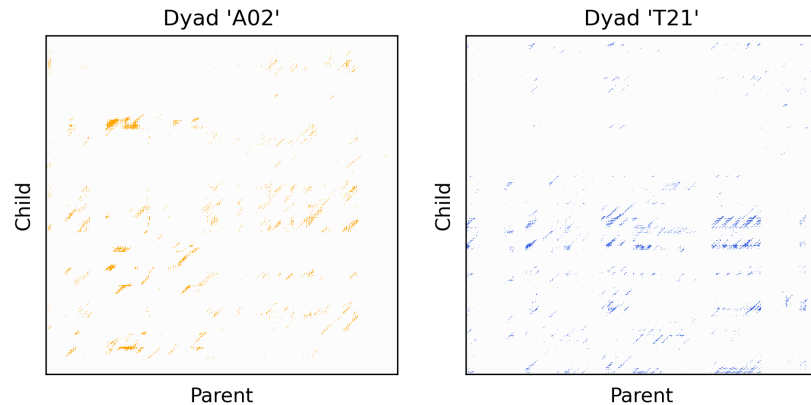


Note. In each plot, arrows point to the first local minima of false nearest neighbors (FNN) ratios and average mutual information (AMI) values of each dyad partner's time series. Optimal time delays (d) of each dyad member are annotated in the top right of each subplot in Panel (b).

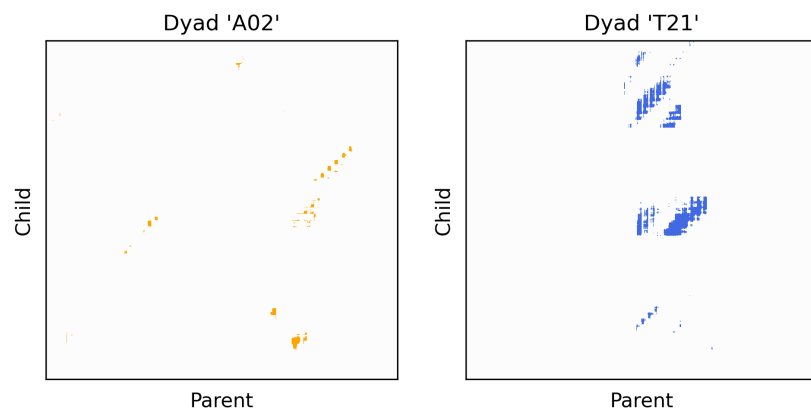
Figure 2

Cross-recurrence plots of parent-child HR and HRV RMSSD values for each dyad

(a)



(b)



Note. Panel (a) shows HR values, and panel (b) shows HRV RMSSD values. Colored dots represent time points at which parent and child heart rate (HR) or HRV RMSSD values are more closely aligned, indicating greater synchrony.